

Published in final edited form as:

*J Med Chem.* 2008 August 14; 51(15): 4430–4448. doi:10.1021/jm701562x.

## Synthesis of GABA<sub>A</sub> Receptor Agonists and Evaluation of their $\alpha$ -Subunit Selectivity and Orientation in the GABA Binding Site

Michaela Jansen<sup>†, #, ^</sup>, Holger Rabe<sup>‡</sup>, Axelle Strehle<sup>§, †, ^</sup>, Sandra Dieler<sup>†</sup>, Fabian Debus<sup>‡</sup>, Gerd Dannhardt<sup>†</sup>, Myles H. Akabas<sup>\*, #</sup>, and Hartmut Lüddens<sup>\*, ‡</sup>

Department of Medicinal Chemistry and Department of Psychiatry, Johannes Gutenberg-University, Mainz, Germany, and Departments of Physiology & Biophysics, Neuroscience and Medicine, Albert Einstein College of Medicine of Yeshiva University, Bronx, New York, USA

### Abstract

Drugs used to treat various disorders target GABA<sub>A</sub> receptors. To develop  $\alpha$  subunit selective compounds, we synthesized 5-(4-piperidyl)-3-isoxazolol (4-PIOL) derivatives. The 3-isoxazolol moiety was substituted by 1,3,5-oxadiazol-2-one, 1,3,5-oxadiazol-2-thione, and substituted 1,2,4-triazol-3-yl heterocycles with modifications to the basic piperidine substituent as well as substituents without basic nitrogen. Compounds were screened by [<sup>3</sup>H]muscimol binding and in patch-clamp experiments with heterologously expressed GABA<sub>A</sub>  $\alpha_i\beta_3\gamma_2$  receptors ( $i = 1-6$ ). The effects of 5-aminomethyl-3*H*-[1,3,4]oxadiazol-2-one **5d** were comparable to GABA for all  $\alpha$  subunit isoforms. 5-piperidin-4-yl-3*H*-[1,3,4]oxadiazol-2-one **5a** and 5-piperidin-4-yl-3*H*-[1,3,4]oxadiazol-2-thione **6a** were weak agonists at  $\alpha_3$ -,  $\alpha_3$ -, and  $\alpha_5$ -containing receptors. When coapplied with GABA they were antagonistic in  $\alpha_2$ -,  $\alpha_4$ -, and  $\alpha_6$ -containing receptors and potentiated  $\alpha_3$ -containing receptors. **6a** protected GABA binding site cysteine-substitution mutants  $\alpha_1$ F64C and  $\alpha_1$ S68C from reacting with methanethiosulfonate-ethylsulfonate. **6a** specifically covalently modified the  $\alpha_1$ R66C thiol, in the GABA binding site, through its oxadiazolethione sulfur. These results demonstrate the feasibility of synthesizing  $\alpha$  subtype selective GABA mimetic drugs.

### Introduction

$\gamma$ -Aminobutyric acid type A receptors (GABA<sub>A</sub>) are responsible for most of the fast inhibitory synaptic transmission in mammalian brain. They belong to the Cys-loop receptor superfamily of ligand-gated ion channels. These receptors are formed by the pentameric assembly of homologous subunits and contain an anion-selective transmembrane channel. Numerous GABA<sub>A</sub> receptor subunits have been identified ( $\alpha_{1-6}$ ,  $\beta_{1-3}$ ,  $\gamma_{1-3}$ ,  $\delta$ ,  $\pi$ ,  $\epsilon$  and  $\theta$ ), all of which are products of separate genes<sup>1-3</sup>. Most GABA<sub>A</sub> receptors contain two  $\alpha$ , two  $\beta$  subunits and either a  $\gamma$  or a  $\delta$  subunit. Recombinant GABA<sub>A</sub> receptors with different subunit isoform composition display differing sensitivity to the endogenous agonist GABA<sup>4</sup>. The GABA<sub>A</sub> receptor subunits exhibit distinct, although overlapping, regional distribution patterns within the brain, with expression patterns changing during pre- to postnatal development<sup>5</sup>. In addition, in neurons expressing multiple receptor isoforms, subunit-selective targeting to distinct cellular

\*To whom correspondence should be addressed. Hartmut Lüddens, Tel.: +49 6131 175372. Fax: +49 6131 175590. Email: lueddens@uni-mainz.de. Myles H. Akabas, Tel.: +1 718 430 3360. Fax: +1 718 430 8819. Email: makabas@aecom.yu.edu.

<sup>†</sup>Department of Medicinal Chemistry, University of Mainz, Germany

<sup>‡</sup>Department of Psychiatry, University of Mainz, Germany

<sup>#</sup>Departments of Physiology & Biophysics, Neuroscience and Medicine, Albert Einstein College of Medicine of Yeshiva University, Bronx, New York, USA

<sup>^</sup>present addresses: MJ, Department of Physiology and Biophysics, Albert Einstein College of Medicine of Yeshiva University, Bronx, New York, USA; AS, Université Louis Pasteur, Strasbourg, France

<sup>§</sup>MJ and HR contributed equally to this study.

domains has been observed<sup>6, 7</sup>. The subunit isoform diversity and brain region specific expression patterns form the basis for the functional and pharmacological heterogeneity of GABAergic neurotransmission. Presently, most drug therapy for anxiety, epilepsy and surgical sedation and often for insomnia targets GABA<sub>A</sub> receptor subtypes non-selectively, but the heterogeneity of the receptors theoretically holds the promise for brain region- or even cell-selective pharmacological intervention which would increase the specificity of the effects and decrease the incidence of undesirable side effects.

Most of the known pharmacological heterogeneity of GABA<sub>A</sub> receptors concerns the sensitivity of the benzodiazepine site that is formed at the interface between the  $\alpha$  and  $\gamma$  subunits<sup>8–10</sup>. Receptors lacking the  $\gamma_2$  subunit or containing the  $\alpha_4$  or  $\alpha_6$  subunits are practically insensitive to benzodiazepine site agonists<sup>11, 12, 13, 14</sup>. The two GABA binding sites are formed at the interfaces between the  $\beta$  and  $\alpha$  subunits. Only a few different structural classes of ligands are known for the GABA binding site, reflecting the strict structural requirements for GABA<sub>A</sub> receptor recognition and activation. To date these GABA binding site agonist compounds display little subunit subtype specificity with gaboxadol forming a class on its own as a “superagonistic” GABA mimetic<sup>15</sup>. A few compounds have been identified which neither bind to the benzodiazepine nor the GABA binding sites and yet still show subtype-selective antagonistic activity, these include furosemide, otherwise known as a Na<sup>+</sup>/K<sup>+</sup>/2Cl<sup>-</sup> cotransporter blocker, that selectively blocks  $\alpha_{(4/6)}\beta_{(2/3)}\gamma_2$  receptors<sup>16, 17</sup>, and clozapine, an atypical antipsychotic drug, that inhibits furosemide-insensitive  $\alpha_1$  containing receptors<sup>18</sup>.

Undesirable side effects, such as sedation and amnesia, often limit the clinical use of benzodiazepines<sup>19</sup>, as well as the use of full agonists and of zero modulators of the GABA recognition site<sup>20</sup>. Different strategies exist to minimize undesirable effects: subtype-selective ligands or partial agonists. Studies with transgenic rodents have helped to dissect the  $\alpha$ -subunit isoforms involved in specific pharmacologic effect of benzodiazepines. For example,  $\alpha_2$ -containing receptors are primarily responsible for anxiolytic effects of benzodiazepines whereas  $\alpha_1$ -containing receptors are more important for the sedative side effects. Current research efforts focused on designing subunit-selective benzodiazepines<sup>21–27</sup>. In general, it seems desirable to have subtype-selective ligands that only act on a certain receptor subtype that is involved in transducing the desired effect and not on other subtypes that are involved in undesired effects. A complementary approach is to develop partial agonists of the GABA recognition site that induce only submaximal activation of specific  $\alpha$ -subunit containing receptors. Under close to complete receptor occupancy, these partial agonists act as inhibitors of full agonists<sup>15</sup>. Partial agonists at the benzodiazepine site have also been investigated<sup>28–30</sup>.

In a previous study we used binding studies on rat brain cryostat sections and patch-clamp experiments with heterologously expressed recombinant GABA<sub>A</sub> receptors to characterize the low-efficacy GABA mimetic 5-(4-piperidyl)isoxazol-3-ol (4-PIOL) (Figure 1) as a weak partial agonist or antagonist depending on the brain area and the GABA<sub>A</sub> receptor composition<sup>31,32</sup>. Therefore we synthesized and functionally characterized different 5-(4-piperidyl)-1,3,4-oxadiazol- and 5-(4-piperidyl)-1,3,4-triazol-derivatives compounds structurally related to 4-PIOL<sup>33</sup>. The effects of other 4-PIOL derivatives on GABA<sub>A</sub> receptors have been studied previously<sup>34–40</sup>. All compounds were screened for efficacy and potency to GABA<sub>A</sub> receptors in native membranes using a [<sup>3</sup>H]muscimol binding assay. Substances inducing changes in [<sup>3</sup>H]muscimol binding in the micromolar concentration range were further analyzed in patch clamp recordings from GABA<sub>A</sub> receptors heterologously expressed in human embryonic kidney (HEK 293) cells. The  $\alpha$  subunit specificity of these compounds was tested in  $\alpha_i\beta_3\gamma_2$  ( $i = 1–6$ ) GABA<sub>A</sub> receptors by measuring the modulation of GABA-induced chloride current and the intrinsic activity of the compounds. We also sought to demonstrate

that the actions of these new compounds were mediated through binding at the GABA-binding sites. We used a variant of the substituted cysteine accessibility method (SCAM) in order to identify the position and orientation of **6a** in the binding site<sup>41</sup>. Residues in the  $\alpha$  subunit that line the GABA binding site have been identified based on the effects of mutations on electrophysiological properties<sup>42–44</sup>, photo-affinity labeling<sup>45</sup> and SCAM<sup>46–48</sup>. They include those aligned with rat  $\alpha_1$  positions F64, R66, S68 and T129. Although crystal structures of GABA<sub>A</sub> receptor binding sites are not yet available, homology models based on the snail acetylcholine binding protein (AChBP) structure provide a reasonable molecular context in which to interpret our results<sup>49</sup>.

## Synthesis

The synthetic procedures for the 5-(4-piperidyl)-1,3,4-oxadiazole- and 5-(4-piperidyl)-1,3,4-triazole-derivatives in this study are depicted in scheme 1 and scheme 2, whereas schemes 3 and 4 depict specific variations of the 4-piperidyl moiety. Here we describe the synthesis of the 4-piperidyl-derivatives as an example. The secondary amine function of 4-piperidine-carboxylic acid ester was either protected with the *t*-butoxycarbonyl (Boc) group using di-*t*-butyldicarbonate and NaHCO<sub>3</sub> in water or triethylamine in methylene chloride (Scheme 1: **1a**) or alkylated using formaldehyde, formic acid or benzylchloride (Scheme 2: **7a, b**). Subsequently, the esters were converted to the corresponding acid hydrazides (Scheme 1: **2a**; Scheme 2: **8a, b**) by refluxing the ester in an excess of hydrazine hydrate. The 1,3,4-oxadiazol-2-ones (Scheme 1: **3a**; Scheme 2: **9a, b**) were prepared by refluxing the hydrazides with N,N'-carbonyldiimidazol (CDI) in the presence of triethylamine in a mixture of THF and DMF. The corresponding 1,3,4-oxadiazol-2-thiones (Scheme 1: **4a**; Scheme 2: **10a, b**) were synthesized by refluxing the hydrazides with carbonyldisulfide in an ethanolic potassium hydroxide solution. Theoretically, oxadiazol-2-ones and -thiones can exist in two tautomeric forms, the amide form and the imino-alcohol form. IR, UV and NMR spectra, however, indicate that they exist predominantly in their amide-form<sup>50</sup>. The hydrazide **2a** was also cyclized with triethoxyethane to yield the 2-methyl-1,3,4-oxadiazol-derivative (Scheme 1: **18**). Reaction of the hydrazide **2a** with benzylisocyanate or benzylisothiocyanate produced the acylated semicarbazide derivatives **12a** and **13a**, which were converted to benzyl-1,3,4-oxadiazoles **14** and **15** by refluxing with NaOH in an aqueous solution (Scheme 1). N-methyl-piperidin-4-yl carboxylic acid hydrazide (**8b**) was reacted with triethoxymethane to yield the 2-unsubstituted 1,3,4-oxadiazol-derivative **11** (Scheme 2). The 4-piperidyl moiety was varied as outlined in Scheme 3 and 4. It was substituted by a 3-piperidyl and a 2-pyrrolidinyl moiety, or residues that lead to derivatives that mimic glycine, sarcosine, alanine and  $\beta$ -alanine (Scheme 3) as well as N-alkylated 4-piperidiny-compounds, dimethylglycine and two compounds without an amine function (Scheme 4). The last step during the synthesis of compounds **5a–g**, **6a–e**, **g**, **16a**, **17a**, and **19** was the removal of the Boc-protective group with hydrogen chloride (Scheme 1 and 3).

## Pharmacology

### [<sup>3</sup>H]Muscimol binding

Compounds were initially screened by probing their ability to compete with [<sup>3</sup>H]muscimol binding to the GABA recognition site in native cortical and cerebellar membranes. We used two concentrations (100  $\mu$ M and 1 mM) of the compounds. This approach allowed us to eliminate compounds with very low binding affinity. Additionally, we compared the binding of [<sup>3</sup>H]muscimol to membranes from two brain structures: cortex, containing  $\alpha_1$ – $\alpha_5$  receptors, and cerebellum, enriched in  $\alpha_1$ - and the exclusive source of  $\alpha_6$ -containing GABA<sub>A</sub> receptors (Table 1), to enable us to detect pronounced differences in subtype selectivity of the compounds.

Of the 28 compounds tested, six fulfilled our criteria for full binding analysis in that, at 100  $\mu\text{M}$ , they inhibited muscimol binding by at least 30% (Table 1). These six included **5a**, **5d**, **5g**, **6a**, **6d** and **19**. For these compounds we determined the  $\text{IC}_{50}$  values for inhibition of [ $^3\text{H}$ ] muscimol binding to cortical and cerebellar membranes (Table 2, 5d Figure 2). **5d** showed the highest affinity with an  $\text{IC}_{50}$  of 1.4  $\mu\text{M}$  and **5a** exhibited the lowest affinity, 183  $\mu\text{M}$  (Table 2). None of the six compounds displayed significant differences between  $\text{IC}_{50}$  determined in cortical vs cerebellar membranes, though compound **5g** showed a significant difference between the pseudo-Hill coefficient determined in cortical vs cerebellar membranes, 0.63 vs 0.92, respectively, whereas no difference in any measure was detected for the other compounds (Table 2).

### HEK293 Electrophysiology

We characterized the functional effects of four compounds on  $\alpha_i\beta_3\gamma_2$  ( $i = 1-6$ )  $\text{GABA}_A$  receptors using patch-clamp experiments with heterologously expressed  $\text{GABA}_A$  receptors. This allowed us to determine directly the  $\text{GABA}_A$  receptor  $\alpha$  subunit specificity for these four compounds identified as the most potent inhibitors in the [ $^3\text{H}$ ]muscimol binding assays described above. Transiently transfected HEK 293 cells co-expressing an  $\alpha$  variant plus  $\beta_2$  and  $\gamma_2\text{S}$  and Enhanced Green Fluorescent Protein (EGFP) were used in these experiments. EGFP fluorescence facilitated the identification of transfected cells for patch clamping. For each compound we applied a series of increasing drug concentrations either alone, to assess the intrinsic agonist activity, or together with the approximate  $\text{EC}_{20}$  to  $\text{EC}_{25}$  concentration of GABA, to determine its GABA-modifying activity. The GABA  $\text{EC}_{20-25}$  concentrations used for the different  $\alpha$  subunits are shown in Table 3.

### Intrinsic agonist activity

**5a** (5-Piperidin-4-yl-3H-[1,3,4]oxadiazol-2-one hydrochloride) and **6a** (5-Piperidin-4-yl-3H-[1,3,4]oxadiazol-2-thione Hydrochloride) showed limited intrinsic activity in  $\alpha_1$ ,  $\alpha_4$ , and  $\alpha_6$  containing receptors (Figure 3). At 1 mM the induced currents were less than 10% of the currents induced by the approximate  $\text{EC}_{100}$  GABA concentrations (Figure 4). In contrast, on  $\alpha_2$ ,  $\alpha_3$ , and  $\alpha_5$  containing receptors, 1 mM **5a** caused currents of  $17 \pm 1\%$ ,  $18 \pm 2\%$ , and  $34 \pm 3\%$  of the maximal GABA-induced currents. On the same receptors 1 mM **6a** induced currents that were  $23 \pm 5\%$ ,  $13 \pm 2\%$ , and  $48 \pm 4\%$  of the maximal GABA-induced currents.

**5d** (5-Aminomethyl-3H-[1,3,4]oxadiazol-2-one hydrochloride) induced desensitizing currents in all  $\text{GABA}_A$  receptor combinations tested in a dose-dependent manner with an efficacy  $>50\%$  of the maximal GABA-induced currents and an  $\alpha$  subunit specific potency (Table 4, Figure 3). Receptors containing  $\alpha_6$  subunits were most sensitive with an  $\text{EC}_{50}$  of 30  $\mu\text{M}$  and receptors containing the  $\alpha_3$  subunit were the least sensitive with a **5d**  $\text{EC}_{50}$  of ca. 2300  $\mu\text{M}$ .

The ability of **19** (4-(5-Methyl-[1,3,4]oxadiazol-2-yl)-piperidine hydrochloride) to directly activate  $\text{GABA}_A$  receptors was restricted to  $\alpha_6$  containing receptors where it induced currents  $29 \pm 4\%$  of the maximal GABA-evoked currents. With all of the other  $\alpha$  subunits 1 mM **19** induced a current less than 10% of the maximal GABA-induced current.

### GABA modulatory effect

**5a** showed a slight dose-dependent potentiating effect on  $\alpha_3$  and  $\alpha_5$  containing  $\text{GABA}_A$  receptors with maximal current potentiation by 1 mM **5a** of  $22 \pm 11\%$  for  $\alpha_3$  and  $34 \pm 5\%$  for  $\alpha_5$  containing receptors (Figure 4). In all other  $\alpha$  subunits its action was antagonistic on GABA-induced currents with similar potency. Its antagonistic efficacy was highest in  $\alpha_1$  containing receptors where 1 mM **5a** inhibited GABA-induced current by  $77 \pm 3\%$ . At this concentration **5a** inhibited GABA-induced currents of other  $\alpha$  subunits by  $42 \pm 2\%$  for  $\alpha_2$ ,  $52 \pm 5\%$  for  $\alpha_4$ , and  $41 \pm 4\%$  for  $\alpha_6$ .

**6a** (5-Piperidin-4-yl-3H-[1,3,4]oxadiazol-2-thione hydrochloride), the thio-derivative of **5a**, had similar effects to **5a** except on  $\alpha_2$  containing receptors. **6a** potentiated GABA-induced currents in  $\alpha_5\beta_3\gamma_2$  receptors to an extent similar to that described for **5a**, but on  $\alpha_3\beta_3\gamma_2$  receptors the potentiating effect of **6a** was higher with a current potentiation of  $114 \pm 8\%$  at 1 mM. In contrast to **5a**, in  $\alpha_2$ -containing receptors, low concentrations of **6a** potentiated submaximal GABA-induced currents with maximal potentiation of  $39 \pm 4\%$  at 1  $\mu$ M. Whereas at 1 mM, **6a** inhibited GABA currents by  $24 \pm 9\%$ . **6a** also inhibited GABA-induced currents in  $\alpha_1$ ,  $\alpha_4$ , and  $\alpha_6$  containing receptors.

**5d**(5-Aminomethyl-3H-[1,3,4]oxadiazol-2-one hydrochloride), potentiated the GABA-induced currents for all of the  $\alpha$  subunit isoforms with similar potency, apparent  $EC_{50}$  values ranged between 100 and 300  $\mu$ M (Figure 3). The efficacy was similar in  $\alpha_1$ ,  $\alpha_2$ ,  $\alpha_3$ , and  $\alpha_4$  containing receptors with current potentiation of  $302 \pm 35\%$ ,  $324 \pm 40\%$ ,  $311 \pm 18\%$ , and  $334 \pm 13\%$  at 1 mM, respectively. The **5d** efficacy was significantly enhanced in receptors comprising  $\alpha_5$  ( $423 \pm 25\%$ ) and  $\alpha_6$  ( $437 \pm 21\%$ ) subunits with  $p$  of  $<0.01$  in a two-sided t-test compared to  $\alpha_1$  containing receptors.

Lastly, we analyzed the GABA<sub>A</sub> receptor  $\alpha$  subunit specificity of **19** (4-(5-methyl-[1,3,4]oxadiazol-2-yl)-piperidine hydrochloride) and its hydrobromide with electrophysiological methods. This novel compound increased the GABA-induced currents in all GABA<sub>A</sub> receptor combinations tested with similar potency. The efficacy shows a slight subtype specificity which could be divided into two significantly different groups with  $p$  of  $<0.01$  in a two-sided t-test. The group with higher efficacy consisting of  $\alpha_2$ ,  $\alpha_4$ ,  $\alpha_5$ , and  $\alpha_6$  with positive modulation of the GABA-induced currents ranging from 48% in  $\alpha_2$  to 87% in  $\alpha_6$  at 1 mM **19**. The positive modulation efficacy was smaller for  $\alpha_3$  and  $\alpha_1$  containing receptors where compound **19** potentiated the GABA-induced currents by  $11\% \pm 2$  and by  $21\% \pm 5$ , respectively.

## Two-Electrode Voltage Clamp Electrophysiology in *Xenopus laevis* oocytes

Based on the diverse set of effects, potentiation, inhibition and direct activation, seen with the compounds we sought to demonstrate that they bound in the GABA binding site. These experiments focused on compound **6a**. We used a series of cysteine-substitution mutants in the GABA binding site.

**Determination of GABA  $EC_{50}$  values**—GABA dose-response relationships were determined for wild type and mutant  $\alpha_1\beta_2$  receptors expressed in *Xenopus* oocytes (Table 5). Mutant  $\alpha_1S68C\beta_2$  receptors had an  $EC_{50}$  value comparable to  $\alpha_1\beta_2$  wt receptors. In contrast, the  $EC_{50}$  values for the mutants  $\alpha_1T129C\beta_2$ ,  $\alpha_1F64C\beta_2$  and  $\alpha_1R66C\beta_2$  were increased 14-fold, 43-fold and 554-fold, respectively, compared to wild type, in agreement with previously published data<sup>46, 47</sup>.

**Determination of **6a**  $EC_{50}$** —**6a** acted as an agonist on  $\alpha_1\beta_2$  wt,  $\alpha_1F64C\beta_2$ , and  $\alpha_1S68C\beta_2$  receptors. To prove that the **6a**-induced currents were mediated by GABA<sub>A</sub> receptor activation we tested the ability of picrotoxinin, an open channel blocker, to inhibit the **6a** induced currents. Co-application of 100  $\mu$ M picrotoxinin and 10 mM **6a** inhibited **6a**-induced currents by 80–90% (Figure 5). We infer that **6a** directly activates GABA<sub>A</sub> receptors.

We determined the **6a**  $EC_{50}$  for the Cys-substitution mutant receptors (Table 5). For wt receptors the **6a**  $EC_{50}$  was 9.5 mM. It was similar for  $\alpha_1S68C\beta_2$ . For  $\alpha_1F64C\beta_2$ , the **6a**  $EC_{50}$  was 0.6 fold less than for wt.

The efficacy of **6a** as compared to GABA was significantly greater for  $\alpha_1F64C\beta_2$  receptors compared to  $\alpha_1\beta_2$  wt and  $\alpha_1S68C\beta_2$ . A 30 mM concentration of **6a** produced currents that were 60, 20, and 17% as large as the maximal GABA current for  $\alpha_1F64C\beta_2$ ,  $\alpha_1\beta_2$  wt, and



$\alpha_1S68C\beta_2$  receptors, respectively. Higher concentrations of **6a** were not used due to the limited supply of the compound. The Hill coefficient of the **6a** dose-response relationship was increased compared to GABA.

**Determination of 6a IC<sub>50</sub> values of the mutants**—Co-application of **6a** and GABA inhibited the GABA-induced currents. We performed competition experiments to determine the **6a** IC<sub>50</sub> for inhibiting GABA EC<sub>20</sub> currents with  $\alpha_1\beta_2$  wt,  $\alpha_1F64C\beta_2$ , and  $\alpha_1S68C\beta_2$  receptors (Table 5). One mM **6a** inhibited the EC<sub>20</sub> GABA current by more than 90% in these receptors. The residual GABA currents observed during the co-application of 1 mM **6a** and GABA EC<sub>20</sub> concentration, were  $6.8 \pm 1.0\%$  ( $n = 4$ ) for  $\alpha_1\beta_2$  wt,  $9.0 \pm 2.0\%$  ( $n = 3$ ) for  $\alpha_1F64C\beta_2$ , and  $3.0 \pm 1.8\%$  ( $n = 6$ ) for  $\alpha_1S68C\beta_2$ . Since the **6a**-GABA competition experiments were done at a relatively low GABA concentration we decided that for the protection experiments the **6a** concentration should be at least 1 mM.

#### **Effects of MTS-reagents on the cysteine mutants and reaction rates—**

Methanethiosulfonate (MTS) reagents react  $10^9$  times faster with ionized thiolates ( $S^-$ ) than with thiols (SH) <sup>51</sup>; thus, they are much more likely to react with water-accessible cysteine, which can ionize. We monitored the MTS reaction with a substituted cysteine by its affect on the channel's macroscopic currents.

Application of the anionic reagent MTS-ethylsulfonate (MTSES<sup>-</sup>) did not affect the GABA current in  $\alpha_1\beta_2$  wt receptors (data not shown) <sup>46</sup>. After complete reaction with MTSES<sup>-</sup> and/or MTSEA-biotin, subsequent GABA EC<sub>50</sub> currents were inhibited to a similar extent for  $\alpha_1F64C\beta_2$ ,  $\alpha_1R66C\beta_2$ ,  $\alpha_1S68C\beta_2$  and  $\alpha_1T129C\beta_2$  receptors (see Table 6). We infer that in the cysteine-substitution mutants, changes in the GABA-induced current after MTS application were due to the covalent modification of the engineered cysteine.

The observed second-order rate constants for reaction with MTSES<sup>-</sup> were  $11300 \pm 700 M^{-1}/s$  for  $\alpha_1F64C\beta_2$ ,  $48 \pm 7 M^{-1}/s$  for  $\alpha_1R66C\beta_2$ , and  $240 \pm 40 M^{-1}/s$  for  $\alpha_1S68C\beta_2$ , which are in agreement with previously reported results (Table 7, Figure 6) <sup>46</sup>. For  $\alpha_1R66C\beta_2$  and  $\alpha_1T129C\beta_2$  the second-order reaction rate constant for MTSEA-biotin with  $\alpha_1R66C\beta_2$  was  $5500 \pm 1600 M^{-1}/s$  and with  $\alpha_1T129C\beta_2$  was  $6,700,000 \pm 1,100,000 M^{-1}/s$  (Table 6). All reaction rates were well fit by a mono-exponential function. For each mutant receptor, however, there are two engineered cysteine residues, because  $\alpha\beta$ -receptors are pentameric and their subunit stoichiometry is proposed to be  $2\alpha:3\beta$  <sup>52, 53</sup>. Either the two cysteine residues from each receptor reacted at the same rate, or reaction at only one residue gave the complete effect. These two possibilities are indistinguishable with the present methods.

**Protection of cysteine mutants by GABA and 6a**—If an engineered cysteine forms part of a ligand-binding site, then the presence of the ligand in the binding site should reduce the ability of MTS reagents to react with the cysteine. This should decrease the measured MTS reaction rate in the presence of the ligand. It was reported previously that in the presence of GABA  $\alpha_1F64C$ ,  $\alpha_1R66C$ , and  $\alpha_1S68C$  are protected from reaction with MTS reagents (MTSEA-biotin, MTSES<sup>-</sup>, MTSEA<sup>+</sup>) <sup>46, 47</sup>. This protection may be due either to direct steric protection due to the presence of GABA in the binding site or to a GABA-induced conformational change reducing the accessibility of these residues to the MTS reagent. The fact that these cysteine mutants were also protected from modification by SR-95531, a competitive antagonist, implies that the mechanism of protection is a steric not an allosteric one <sup>46, 47</sup>.

$\alpha_1F64C\beta_2$  and  $\alpha_1S68C\beta_2$  receptors were protected from reaction with MTSES<sup>-</sup> by both GABA and **6a** (Figure 7 and 8). In control experiments with  $\alpha_1F64C\beta_2$ , a 12 s application of 10  $\mu M$  MTSES<sup>-</sup> caused an  $87 \pm 3\%$  ( $n = 4$ ) reduction in subsequent GABA EC<sub>50</sub> test currents (Figure

7A). In contrast, a 12 s co-application of 10  $\mu\text{M}$  MTSES<sup>-</sup> with 3.6 mM GABA caused only a  $35 \pm 1\%$  ( $n = 5$ ) reduction of the subsequent GABA-induced currents (Figure 7B) and co-application of 10  $\mu\text{M}$  MTSES<sup>-</sup> with 10 mM **6a** resulted in only a  $47 \pm 6\%$  ( $n = 4$ ) reduction (Figure 7C) of the subsequent GABA-induced currents. Thus, the extent to which MTSES<sup>-</sup> could react with  $\alpha_1\text{F64C}\beta_2$  was reduced by the presence of GABA and **6a**. This implies that both agonists protected the engineered cysteine from covalent modification.

Similarly for the  $\alpha_1\text{S68C}\beta_2$  mutant, application of 450  $\mu\text{M}$  MTSES<sup>-</sup> for 12 s reduced the subsequent GABA test currents by  $77 \pm 5\%$  ( $n = 4$ ) (Figure 8). Co-application of 450  $\mu\text{M}$  MTSES<sup>-</sup> with 65  $\mu\text{M}$  GABA or 10 mM **6a** only reduced the subsequent GABA test currents by  $40 \pm 2\%$  ( $n = 4$ ) and  $10 \pm 4\%$  ( $n = 4$ ), respectively, consistent with protection of the  $\alpha_1\text{S68C}$  cysteine residue.

In similar experiments with  $\alpha_1\text{R66C}\beta_2$  receptors, 10 mM **6a** demonstrated slight, but significant protection of the engineered cysteine from reaction with MTSES<sup>-</sup> (Figure 8). A 12 s application of 2 mM MTSES<sup>-</sup> to  $\alpha_1\text{R66C}\beta_2$  inhibited  $91 \pm 3\%$  ( $n = 6$ ) of the subsequent GABA EC<sub>50</sub> current. Co-application of 35 mM GABA with MTSES<sup>-</sup> inhibited  $49 \pm 6\%$  ( $n = 3$ ) of the subsequent test currents, consistent with protection by GABA. In contrast, application of 10 mM **6a** with 2 mM MTSES<sup>-</sup> resulted in  $77 \pm 4\%$  ( $n = 5$ ) inhibition of the subsequent GABA test currents. Comparable results were obtained for MTSEA-biotin, application of 30 mM **6a** with MTSEA-biotin resulted in 79 and 87% ( $n = 2$ ) inhibition of the subsequent GABA test currents as compared to 87 and 100% ( $n = 2$ ) inhibition in control experiments. For  $\alpha_1\text{R66C}$  the results of the protection experiments are complicated by the fact that **6a** reacts with  $\alpha_1\text{R66C}\beta_2$  as described below.

**6a reacts with the engineered cysteine in  $\alpha_1\text{R66C}\beta_2$  receptors**—To our surprise, while examining competition between GABA and **6a** on  $\alpha_1\text{R66C}\beta_2$  receptors, we noted that once the oocytes showed stable GABA test responses, co-application of GABA and **6a** irreversibly reduced the subsequent GABA test currents (data not shown). Alternating between GABA and **6a** resulted in a progressive decline in the GABA test currents that finally led to a stable GABA current that was significantly lower,  $68 \pm 4\%$  ( $n = 4$ ), than the initial GABA test current (Figure 9A). At this stage, application of MTSES<sup>-</sup> caused no further effect. In contrast, application of MTSES<sup>-</sup> to  $\alpha_1\text{R66C}\beta_2$  expressing oocytes untreated with **6a** produced  $62 \pm 3\%$  ( $n = 4$ ) inhibition of GABA currents. Furthermore, the GABA currents after either **6a** or MTSES<sup>-</sup> application could be recovered by application of the reducing agent DTT (10 mM, 20 s) (Figure 9A). Theoretically, oxadiazole-2-thiones, such as **6a**, can exist in two tautomeric forms, the thio-amide (thione) form and the imino-thiol form. IR, UV and NMR spectra indicate that they do exist predominantly in their thione-form<sup>50</sup>. However, the ability to form the thiol-tautomer enables the oxadiazole-2-thione to form a disulfide bond. Consistent with the idea of the formation of a stable disulfide bond, repeated 10 s applications of 30 mM **5a**, a **6a** analogue with an oxygen in place of the potentially sulfhydryl reactive oxadiazolethione sulfur moiety, did not irreversibly alter the subsequent GABA currents in  $\alpha_1\text{R66C}\beta_2$  expressing oocytes (Figure 9B).

In order to measure the reaction rate of **6a** with  $\alpha_1\text{R66C}$  we alternately applied 5.5 mM GABA and **6a** to oocytes until the GABA currents no longer declined (Figure 9A). The decline in the  $\alpha_1\text{R66C}\beta_2$  GABA currents as a function of the cumulative **6a** exposure time could be fit with a single exponential decay function. **6a** second-order reaction rate with the engineered cysteine in  $\alpha_1\text{R66C}$  was  $5 \pm 1 \text{ M}^{-1}/\text{s}$  ( $n = 3$ ) (Figure 9A, C). The second-order reaction rate constant was independent of the **6a** concentration used (either 10 or 30 mM).

In our homology model based on the AChBP structure the  $\alpha_1$  subunit residues R66 and T129 are in close proximity but on adjacent  $\beta$ -strands. Based on protection with agonist and

antagonist SCAM analysis predicts that  $\alpha_1$ T129 lines the binding pocket<sup>48</sup>. A 2-min application of 5 mM MTSES<sup>-</sup> reduced the subsequent currents elicited by GABA EC<sub>50</sub> test pulses in  $\alpha_1$ T129C $\beta_2$  by  $63 \pm 5\%$  ( $n = 3$ ). We tested whether **6a** would react with  $\alpha_1$ T129C. Alternate application of EC<sub>50</sub> GABA and 30 mM **6a** did not lead to a change in GABA EC<sub>50</sub> peak currents in  $\alpha_1$ T129C $\beta_2$ ,  $\alpha_1$ F64C $\beta_2$ , or  $\alpha_1$ S68C $\beta_2$  containing receptors, suggesting that the reaction of **6a** with  $\alpha_1$ R66C is highly specific. It should be noted that the MTSES<sup>-</sup> reaction rate with  $\alpha_1$ R66C was at least 5-fold slower than with any of the other cysteine mutants used in this study (Table 6). It was orders of magnitude slower than the reaction rate with  $\alpha_1$ T129C. Thus, the lack of **6a** reaction with the other cysteine mutants is not due to lower intrinsic reactivity of those positions.

## Discussion

### Structure-Activity relationships of 1,3,4-oxadiazol-2-ones

The 1,3,4-oxadiazol-2-one compound with the highest affinity as measured by inhibiting muscimol binding is the aminomethyl-derivative **5d** with IC<sub>50</sub> values of 1.4  $\mu$ M and 1.1  $\mu$ M against rat cortex and cerebellum, respectively. The homo-derivative **5g** with its 2-aminoethyl side chain displayed seven times higher IC<sub>50</sub> values. The conversion of the primary amine function of **5d** to a secondary methylaminomethyl group in **5e** caused a significant decrease in affinity and the tertiary dimethylaminomethyl compound **9c** showed negligible capacity to displace [<sup>3</sup>H]muscimol. Thus, the affinity among the 5-aminomethyl-3*H*-[1,3,4]oxadiazol-2-ones decreases from the primary aminomethyl **5d** over the secondary methylaminomethyl **5g** to the tertiary dimethylaminomethyl **9c**. We infer that the amino group is involved in interactions with the binding site because the cyclohexyl- **9d** and methyl **9e** substituted oxadiazol-2-ones that lack an amino group do not show significant inhibition of muscimol binding.

An additional steric demand at the methylene group of the aminomethyl compound **5d** that led to the 1-aminoethyl derivative **5f** was not well tolerated, i.e., the methyl group in **5f** led to a significant decrease in the ability to displace [<sup>3</sup>H]muscimol. The 2-pyrrolidine compound **5c**, which can be considered as a bridged aminomethyl derivative of **5d**, showed an almost complete loss of affinity. In **5c** the inhibition reducing effects of a secondary amine function and a steric strain added to the methylene group are combined. Similarly, when the 2-aminoethyl sidechain was incorporated into a 3-piperidyl ring as in **5b**, the compound was inactive. However, the 4-piperidyl compound **5a**, was active although the IC<sub>50</sub> was increased by a factor of four when compared to the 2-aminoethyl compound **5g**. Thus, the affinity appears to be sensitive to the position of the amino group because when it is at the 4 position in the piperidyl ring as in **5a** the IC<sub>50</sub> was 183  $\mu$ M but when located at the 3 position in **5b** the affinity was negligible. Furthermore, derivatives of the 4-piperidyl amino group leading to tertiary amines in the form of the N-benzyl-piperidine **9b** or the N-methyl-piperidine **9a**, showed weak activity in this assay. This is consistent with the loss of activity as the amino group transits from a primary to secondary to tertiary amino group.

**Structure-Activity relationships of 1,3,4-oxadiazol-2-thiones**—The 4-piperidyl derivative **6a** showed an IC<sub>50</sub> comparable to the aminomethyl derivative **6d**. This is in contrast to the oxadiazolones where the aminomethyl derivative showed a 40 times lower IC<sub>50</sub> than the 4-piperidyl derivative. The aminoethyl derivative **6g** showed the third highest degree of inhibition in the thione series. However, when the aminomethyl or aminoethyl was bridged in the thione series to obtain a 2-pyrrolidinyl **6c** or 3-piperidinyl **6b** compound a significant amount of affinity was still retained. This is also different from the oxadiazolones where the corresponding modifications were not tolerated. Another difference was found when comparing the primary, secondary and tertiary aminomethyl compounds. Here the primary



aminomethyl **6d** had a higher affinity than the dimethylaminomethyl compound **10c** which in turn had a higher affinity than the methylaminomethyl compound **6e**. This decline in affinity seems to be correlated to the basicity. We infer that the amine-N interacts with the protein. Other side chains that resulted in a weak affinity are the compounds with the 4-(N-methyl-piperidinyl) **10a** and the 4-(N-benzyl-piperidinyl) **10b** moiety. Again the cyclohexyl- and methyl substituted oxadiazol-2-thiones **10d** and **10e** did not show a significant inhibition of muscimol binding.

**Structure-activity relationships of modifications to the 1,3,4-oxadiazol-2-one ring itself**—As mentioned above, substituting the 2-one oxygen with sulfur did not have a uniform effect. Depending on the amine-side chain in position 5 of the heterocycle the sulfur bearing compound exhibited lower (4-piperidinyl, **6a** < **5a**; 3-piperidinyl, **6b** < **5b**; 2-pyrrolidinyl, **6c** < **5c**) or higher  $IC_{50}$  values (aminomethyl, **6d** > **5d**; 2-aminoethyl, **6g** > **5g**; methylaminomethyl, **6e** > **5e**) than their oxygen bearing counterparts. For other side chains there was no difference in affinity detected between -thione and -one (N-methyl-piperidine, **9a** = **10a**; N-benzyl-piperidine, **9b** = **10b**). The 4-piperidinyl series **5a**, **6a**, **19** showed, that the hydrogens of the oxadiazol-2-one/oxadiazol-2-thione 3-nitrogen or of the tautomeric oxadiazol-2-ol/oxadiazol-2-thiol 2-alcohol/2 thioalcohol oxygen/sulfur are unlikely to be directly involved in hydrogen-bonding, nor, in their deprotonated form, in ion-ion or ion- $\pi$  interactions, since the 2-methyl-1,3,4-oxadiazole showed intermediate affinity. Moreover, we infer that the heteroatoms in the 1,3,4-oxadiazol ring act as hydrogen-bond acceptors when interacting with amino acids in the binding site. However, the drop in affinity from **6a** over **19** to **5a** followed the decrease in volume of the 2-substituent of the 1,3,4-oxadiazol (sulfur >  $CH_3$  > oxygen). The compound with the smallest substituent (hydrogen) at position 2 of the 1,3,4-oxadiazol **11** showed a complete loss of affinity opposite to the derivatives with an oxygen **9b** or sulfur **10b**, again indicating that some bulk at the 2-position is necessary.

The 1,2,4-triazoles explore the effect of substituting the oxygen at position 1 of the 1,3,4-oxadiazol-ones/thiones with a benzyl substituted nitrogen. This exchange was not tolerated at all in the aminomethyl compound: the triazole **16d** completely lost its affinity in contrast to the 1,3,4-oxadiazol-2-one, whereas the 4-piperidinyl triazole **16a** showed a reduced but still significant displacement of [ $^3H$ ]muscimol. The difference in tolerance of bulk at this position of the heterocyclic half of the compounds might indicate that the longer piperidine derivatives share the binding partners for the side chain amino-N with the shorter ligands, but bridge to different amino acids of the binding site with the heterocyclic portion of the molecule. This difference in coordination might account for the difference in tolerance for bulky substituents.

**Comparison with previous 4-PIOL derivatives**—Frølund and colleagues have reported on the synthesis and evaluation of 4-PIOL derivatives as GABA partial agonists or antagonists. They mainly investigated the influence of substituents at position 4 of the 3-isoxazolol ring<sup>39, 54</sup>. In these studies, small aliphatic and also bulky aromatic substituents were tolerated. 4-PIOL derivatives in these investigations had a  $K_i$  between 0.049 and 10  $\mu M$  as compared to 4-PIOL with 9.1  $\mu M$  and our best derivatives with an  $IC_{50}$  between 1 and 183  $\mu M$ . Methyl or ethyl substitution of 4-PIOL lead to compounds that retained some agonistic activity with the binding affinity as determined by [ $^3H$ ]muscimol binding assays being retained as well, whereas the bulky substituents did not show agonistic activity but their affinity was increased in the binding assays. In the context of the 1,3,4-oxadiazol-2-ol moiety used in the present study, substitution of the oxygen at position 1 with a benzyl substituted nitrogen did not improve affinity as **16a** had a somewhat lower affinity than **5a**. We infer that the large cavity that has been suggested to accommodate the aromatic residues of the 4-substituted 4-PIOL derivatives, is not available for compounds of our series, possibly because the 1,3,4-triazol-2-ol derivatives are not arranged in a way that would align the aromatic moiety with the hydrophobic pocket. It is likely that the occupancy of this cavity by the aromatic substituted 4-PIOL derivatives

prevents the binding site closure which has been proposed to be an early step in the conformational change linking ligand binding to channel gating.

It has been observed previously that the exchange of an oxygen in the small carboxyl group bioisosteric ring by a sulfur can have different effects: the sulfur analogue of 4-PIOL has a higher affinity than 4-PIOL, whereas the sulfur analogue of THIP has a lower affinity than the oxygen containing counterpart<sup>40, 54, 55</sup>. The conclusion was that the 3-isoxazolol heterocycles of 4-PIOL and THIP are not at identical positions in the binding sites. Further results demonstrated that the flexible side chain of the arginine R66 in the  $\alpha_1$  subunit might enable the binding pocket to adapt to different bioactive conformations of ligands<sup>54</sup>.

**$\alpha$ -subunit specificity**—The electrophysiological characterization of the most active compounds was divided in investigating the agonistic potency of individual compounds and determining their modulating effect on GABA-induced currents. The agonistic profiling yielded **5d** as the most active compound. This compound had an EC<sub>50</sub> comparable to the GABA EC<sub>50</sub> at all  $\alpha_1$ - $\beta_3\gamma_2$  subunit combinations, ranging between from 30  $\mu$ M for  $\alpha_6$  to 1 mM for  $\alpha_3$ -containing receptors. In the GABA current modulating assay **5d** showed potentiating effects at all subunit combinations reflecting its pure agonistic character. We assume that the small **5d** compound can be accommodated in all binding sites irrespective of the specific  $\alpha$  subunit where its orientation and size allow complete agonist-induced contraction of the binding site and subsequent gating in a manner comparable to the GABA induced effect. Increasing the spacer that bridges the basic amino function from the oxadiazolol moiety from a methylene group in **5d** to a piperidine ring in **5a** converts the compound from an unselective agonist into an antagonist at  $\alpha_1$ ,  $\alpha_4$ , and  $\alpha_6$  containing receptors and a weak partial agonist at  $\alpha_2$ ,  $\alpha_3$  and  $\alpha_5$  containing receptors. The intrinsic activity is highest at  $\alpha_5$  containing receptors. The thio derivative of **5a**, **6a**, showed a comparable profile, with the exception that at  $\alpha_2$  containing receptors it is potentiating GABA currents at low concentrations while it is inhibitory at higher concentrations. The methyl derivative **19** was only agonistic at  $\alpha_6$  receptors, while it showed slight potentiating effects at high concentrations at  $\alpha_2$ ,  $\alpha_4$ ,  $\alpha_5$  and  $\alpha_6$  containing receptors.

**6a binds in the GABA binding site**—Numerous drugs modulate and directly activate GABA<sub>A</sub> receptors often by binding to sites other than the GABA binding sites. Based on several lines of evidence we conclude that **6a** binds within the GABA binding pocket. First, **6a** protected  $\alpha_1$ F64C and  $\alpha_1$ S68C from modification by MTSES<sup>-</sup> (Fig. 7 and 8). These residues are located in the GABA binding site in a homology model based on the AChBP structure 49, 56–58. Czajkowski and coworkers previously showed that GABA protected the cysteine at  $\alpha_1$ F64C from modification by MTSES<sup>-</sup> but pentobarbital did not. Pentobarbital activates the receptor by binding at a site in the transmembrane domain. Thus, the lack of protection by pentobarbital argues that the protection induced by GABA is due to local steric effects of GABA and not due to conformational changes associated with gating<sup>46, 47</sup>. Thus, we conclude that **6a** protected  $\alpha_1$ F64C by its presence in the GABA binding site and not by conformational changes induced by **6a** binding. Secondly, **6a** specifically and covalently modified the neighboring cysteine-substitution mutant,  $\alpha_1$ R66C, inhibiting the subsequent GABA currents. This inhibition did not occur with **5a** which has an oxygen in place of the thiol-reactive sulfur in **6a**. Furthermore, following inhibition of  $\alpha_1$ R66C by reaction with **6a** subsequent application of MTSES<sup>-</sup> had no effect, whereas, without **6a** pretreatment, application of MTSES<sup>-</sup> would have inhibited the GABA-induced currents. Thus, MTSES<sup>-</sup> had no effect when it was applied after **6a** because MTSES<sup>-</sup> cannot react with disulfide linked sulfurs. In contrast, the inhibition induced by **6a** reaction was reversed by DTT application indicating that **6a** formed a mixed disulfide bond with the cysteine thiol. Taken together, we infer that **6a** binds in the GABA binding site.

The ability of **6a** to protect  $\alpha_1$ S68C from modification by MTSES<sup>-</sup> provides insight into the conformational changes induced by **6a** binding (Fig. 8). Both GABA and pentobarbital protected this cysteine mutant from MTSES<sup>-</sup> modification. Czajkowski and coworkers concluded that in the activated state conformation, access to this residue was reduced due to a conformational change of the binding site rather than by the presence of GABA in the binding site<sup>59</sup>. We infer that in the region of  $\alpha_1$ S68 **6a** produces a similar conformational change to that induced by GABA and pentobarbital when it activates the receptor. This suggests that **6a** induces a conformational change in the receptor similar to that induced by GABA binding.

Further, the disulfide bond formation between **6a** and the introduced cysteine at the  $\alpha_1$ R66 position provides insight into the orientation of **6a** in the GABA binding site. The reaction between **6a** and  $\alpha_1$ R66C appears to be specific because **6a** did not react at a measurable rate with the cysteine substituted for the neighboring residues on the same  $\beta$  strand,  $\alpha_1$ F64 or  $\alpha_1$ S68, nor did it react with a cysteine at  $\alpha_1$ T129, the residue predicted to lie in closest proximity on the adjacent  $\beta$  strand. If all other factors were similar, the ratio of the reaction rates of **6a** with the four cysteine mutants should be similar to the ratio of the reaction rates for the MTS reagents with these mutants. The MTS reagents reacted faster with  $\alpha_1$ F64C and  $\alpha_1$ S68C than with  $\alpha_1$ R66C (Table 6). Thus, it is surprising that **6a** only reacted at a measurable rate with  $\alpha_1$ R66C. Since **6a** is much less reactive than the MTS reagents the reason why this compound only reacts at this position must be attributed to a highly selective interaction of the **6a** sulfur with the  $\alpha_1$ R66C sulfur. Therefore, we infer that the favorable orientation of **6a** in the binding site brings the **6a** sulfur into close proximity with the  $\alpha_1$ R66 position leading to the highly specific reaction. This establishes one point of contact between **6a** and the complementary side of the binding site.

We assume that **6a** bridges the principle and complementary sides of the binding site in a manner similar to GABA. We generated a model of the GABA<sub>A</sub> receptor  $\beta_2$ - $\alpha_1$  interface based on the AChBP crystal structure with nicotine bound (Figure 10). **6a** can fit into the binding site with its basic nitrogen superposed on the position of nicotine's basic pyridine nitrogen in the principle side of the binding site and with the **6a** sulfur in close proximity to the introduced  $\alpha_1$ R66C sulfur on the complementary side of the binding site (Figure 10B). The close proximity of the sulfurs may explain the high collision probability and consequently the reactivity necessary to form the disulfide bond between **6a** and the engineered cysteine at position  $\alpha_1$ R66. This orientation in the binding site may explain why it is a weak agonist. In the AChBP crystal structure on the complementary side of the binding site, nicotine forms hydrogen bonds with backbone carbonyls and amides on the  $\beta$  strand containing the residue that aligns with  $\alpha_1$ T129 (Figure 10C). This  $\beta$  strand is adjacent to the  $\alpha_1$ R66-containing  $\beta$  strand. **6a** is larger than GABA: the distance between the two potential H-bonding sites, i.e., the protonated positively charged nitrogen and the most distant high electron dense heteroatom O (GABA) and S (**6a**) (Figure 11 and 10), being 6.1 Å and 7.6 Å, respectively. Thus, GABA might only span the distance between the  $\beta$ -subunit principle site residues where the positively charged N is coordinated and the  $\alpha_1$ T129  $\beta$ -strand of loop E (Figure 10A). In contrast, the larger **6a** extends to the more distant  $\beta$  strand containing residue  $\alpha_1$ R66 (Figure 10B). Activation of the Cys-loop receptors may involve a contraction of the two halves of the binding site<sup>59</sup>. Because **6a** bridges to a different part of the complementary side of the binding site its ability to pull the two halves of the binding site together may be reduced compared to GABA resulting in **6a** being a partial agonist. The idea that **6a** is a partial agonist because it is less effective at closing the binding site is consistent with the conceptual model of partial agonism derived from structural studies of the ionotropic glutamate receptors<sup>60</sup>.

**6a** should not cover the  $\alpha_1$  loop connecting L117 and L127 that harbors the four amino acids (ITED in  $\alpha_1$ ) recently identified as  $\alpha$  variant specific transducing elements rather than binding site elements<sup>4</sup>. A trap-like motion of this loop, to an extent specified by these four amino acids

in a given  $\alpha$  isoform, could further explain the differences in GABA sensitivities between the GABA<sub>A</sub> receptor subtypes.

## Conclusions

We synthesized a series of derivatives of 4-PIOL, a compound previously shown to be a weak GABA<sub>A</sub> partial agonist. We started by replacing the 3-isoxazolol moiety in 4-PIOL with a 1,3,5-oxadiazol-2-ol moiety to yield **5a**. For the first time we describe GABA<sub>A</sub> receptor ligands with a 1,3,5-oxadiazol-2-ol as a carboxylic acid bio-isosteric group. Compound **5a** was modified at different positions to investigate structure-activity relationships: the piperidine moiety was exchanged and modified, the substituent at the 2 position of the 1,3,5-oxadiazol-2-ol was varied, and the 1,3,5-oxadiazol-2-ol was exchanged by 1,2,4-triazol-5-ol.

The most active piperidine derivatives **5a** and **6a** were weak partial agonists that differentiated weakly between different  $\alpha$  subunit containing receptors, whereas the small aminomethyl **5d** showed a profile of a pure agonist that is very similar to GABA.

The described structure-activity relationships extend the currently available information for ligands of the agonist binding site of the GABA<sub>A</sub> receptor. Frølund et al. have shown previously how to convert 4-PIOL into pure antagonistic compounds while we now show how 4-PIOL can be modified to either obtain a pure or partial agonists with weak  $\alpha$  subtype preferring profiles.

In addition, this study demonstrates that **6a** binds in the GABA binding site, and that **6a** is oriented in the binding site such that its interaction with the complementary portion of the binding site is displaced from the interaction site of nicotine and carbamylcholine in the AChBP structure. The later finding may explain why **6a** is a partial agonist. Further investigations are necessary to determine if the two GABA binding sites are the only sites involved in the activity of this compound. These results coupled with GABA binding site homology models based on the AChBP structure may provide a foundation for rational design of GABA<sub>A</sub> receptor subtype-specific agonists with higher efficacy and specificity.

## Experimental Section

### Chemistry

Procedures and spectroscopic data for non-target compounds can be found in the supporting information.

**General Procedures for the Removal of the Boc-group: Procedure F (Compounds 5a,c,e,f,g, 6c,d,e,f,g, 16a,d, 17a, 19)**—The Boc-protected amine (1 equiv) was dissolved in a minimum amount of methanol and cooled in an ice-bath in a nitrogen atmosphere. After adding ethanolic HCl 2.3N (4.5 equiv) the mixture was allowed to reach room temperature and stirred overnight. Products were isolated by filtration in a nitrogen atmosphere, in some cases a precipitate was only formed after adding ethyl acetate (50–98%).

**Procedure G (Compounds 5b,d, 6a,b, 19)**—The Boc-protected amine was dissolved in ethyl acetate and cooled to  $-20^{\circ}\text{C}$  in a nitrogen atmosphere. Gaseous HCl was bubbled through the mixture for 5 min. The reaction was allowed to come to room temperature and stirred until a precipitate was formed. Products were isolated by filtration in a nitrogen atmosphere, or after removing the solvent and recrystallization in ethanol (56–88%).

**5-Piperidin-4-yl-3H-[1,3,4]oxadiazol-2-one Hydrochloride. (5a)**—Starting from **3a** the compound was synthesized as described in procedure F: white crystals (98%); mp =  $314^{\circ}$

C;  $^1\text{H}$  NMR (DMSO- $d_6$ )  $\delta$  1.74–1.88 (m, 2H, 2CH), 2.00–2.05 (m, 2H, 2CH), 2.89–3.03 (m, 3H, 3CH), 3.21–3.25 (m, 2H, 2CH), 8.98–9.28 (m, 2H,  $\text{NH}_2$ ), 12.26 (s, 1H, NH);  $^{13}\text{C}$  NMR (DMSO- $d_6$ )  $\delta$  24.75 ( $\text{CH}_2$ ), 30.94 (CH), 42.07 ( $\text{CH}_2$ ), 155.11 (Cq), 158.08 (Cq); EI-MS  $m/z$  169 ( $\text{M}^+$ ). Anal. ( $\text{C}_7\text{H}_{11}\text{N}_3\text{O}_2\cdot\text{HCl}$ ) C, H, N.

**5-Piperidin-3-yl-3H-[1,3,4]oxadiazol-2-one Hydrochloride. (5b)**—Starting from **3b** the compound was synthesized as described in procedure G. The solvent was removed under reduced pressure and the residue recrystallized from ethanol: white crystals (66%); mp = 207 °C;  $^1\text{H}$  NMR (DMSO- $d_6$ )  $\delta$  1.60–1.85 (m, 3H, 3CH), 1.97–2.01 (m, 1H, 1CH), 2.82–2.91 (m, 1H, 1CH), 2.96–3.04 (m, 1H, 1CH), 3.13–3.19 (m, 2H, 2CH), 9.26 (m, 2H,  $\text{NH}_2$ ), 12.32 (s, 1H, NH);  $^{13}\text{C}$  NMR (DMSO- $d_6$ )  $\delta$  24.75 ( $\text{CH}_2$ ), 30.94 (CH), 42.07 ( $\text{CH}_2$ ), 155.11 (Cq), 158.08 (Cq); MS  $m/z$  167 ( $\text{M}^+$ -2 free base). Anal. ( $\text{C}_7\text{H}_{11}\text{N}_3\text{O}_2\cdot\text{HCl}$ ) C, H, N.

**L-5-Pyrrolidin-2-yl-3H-[1,3,4]oxadiazol-2-one Hydrochloride. (5c)**—Starting from **3c** the compound was synthesized as described in procedure F: white crystals (84%); mp = 199 °C;  $^1\text{H}$  NMR (DMSO- $d_6$ )  $\delta$  1.88–2.05 (m, 2H, 2CH), 2.12–2.30 (m, 2H, 2CH), 3.20–2.25 (m, 2H, CH), 4.63 (t, 7.75 Hz, 1H, CH), 10.13 (s, 2H,  $\text{NH}_2$ ), 12.72 (s, 1H, NH);  $^{13}\text{C}$  NMR (DMSO- $d_6$ )  $\delta$  23.77 ( $\text{CH}_2$ ), 27.18 ( $\text{CH}_2$ ), 45.56 ( $\text{CH}_2$ ), 52.88 (CH), 152.34 (Cq), 154.72 (Cq); EI-MS  $m/z$  155 ( $\text{M}^+$  free base);  $[\alpha]_D^{25} = -3.9^\circ$  (RT,  $c = 0.71$ ,  $\text{H}_2\text{O}$ ). Anal. ( $\text{C}_6\text{H}_9\text{N}_3\text{O}_2\cdot\text{HCl}$ ) C, H, N.

**5-Aminomethyl-3H-[1,3,4]oxadiazol-2-one Hydrochloride. (5d)**—Starting from **3d** the compound was synthesized as described in procedure G. The product was separated by filtration after stirring a few minutes at room temperature: white crystals (88%); mp = 235 °C;  $^1\text{H}$  NMR (DMSO- $d_6$ )  $\delta$  4.03 (s, 2H,  $\text{CH}_2$ ), 8.82 (s, 3H,  $\text{CH}_2\text{NH}_3$ ), 12.71 (s, 1H, NH); EI-MS  $m/z$  115 ( $\text{M}^+$  free base). Anal. ( $\text{C}_3\text{H}_5\text{N}_3\text{O}_2\cdot\text{HCl}$ ) C, H, N.

**5-Methylaminomethyl-3H-[1,3,4]oxadiazol-2-one Hydrochloride (5e)**—Starting from **3e** the compound was synthesized as described in procedure F: white crystals (79%); mp = 176 °C;  $^1\text{H}$  NMR (DMSO- $d_6$ )  $\delta$  2.58 (s, 3H,  $\text{CH}_3$ ), 4.15 (s, 2H,  $\text{CH}_2$ ), 9.88 (s, 2H,  $\text{NH}_2$ ), 12.81 (s, 1H, NH);  $^{13}\text{C}$  NMR (DMSO- $d_6$ )  $\delta$  32.75 ( $\text{CH}_2$ ), 42.22 ( $\text{CH}_3$ ), 150.10 (Cq), 154.65 (Cq); EI-MS  $m/z$  129 ( $\text{M}^+$  free base). Anal. ( $\text{C}_4\text{H}_7\text{N}_3\text{O}_2\cdot\text{HCl}$ ) C, H, N.

**D-5-(1-Amino-ethyl)-3H-[1,3,4]oxadiazol-2-one Hydrochloride. (5f)**—Starting from **3f** the compound was synthesized as described in procedure F: white crystals (90%); mp = 194 °C;  $^1\text{H}$  NMR (DMSO- $d_6$ )  $\delta$  1.47 (d, 6.86 Hz, 3H,  $\text{CH}_3$ ), 4.44 (q, 6.86 Hz, 1H, CH), 8.93 (2, 3H,  $\text{NH}_3$ ), 12.75 (s, 1H, NH);  $^{13}\text{C}$  NMR (DMSO- $d_6$ )  $\delta$  15.77 ( $\text{CH}_3$ ), 42.62 ( $\text{CH}_2$ ), 154.16 (Cq), 154.67 (Cq); EI-MS  $m/z$  129 ( $\text{M}^+$  free base);  $[\alpha]_D^{25} = +7.0^\circ$  (RT,  $c = 0.63$ ,  $\text{H}_2\text{O}$ ). Anal. ( $\text{C}_4\text{H}_7\text{N}_3\text{O}_2\cdot\text{HCl}$ ) C, H, N.

**[5-(2-Amino-ethyl)-3H-[1,3,4]oxadiazol-2-one Hydrochloride. (5g)**—Starting from **3g** the compound was synthesized as described in procedure F: white crystals (77%); mp = 206 °C;  $^1\text{H}$  NMR (DMSO- $d_6$ )  $\delta$  2.89 (t, 6.60 Hz, 2H,  $\text{CH}_2\text{CH}_2\text{NH}_3$ ), 3.06 (t, 6.74 Hz, 1H,  $\text{CH}_2\text{CH}_2\text{NH}_3$ ), 8.23 (s, 3H,  $\text{NH}_3$ ), 12.25 (s, 1H, NH);  $^{13}\text{C}$  NMR (DMSO- $d_6$ )  $\delta$  24.49 ( $\text{CH}_2$ ), 35.37 ( $\text{CH}_2$ ), 153.97 (Cq), 155.27 (Cq); EI-MS  $m/z$  129 ( $\text{M}^+$  free base). Anal. ( $\text{C}_4\text{H}_7\text{N}_3\text{O}_2\cdot\text{HCl}$ ) C, H, N.

**5-Piperidin-4-yl-3H-[1,3,4]oxadiazol-2-thione Hydrochloride. (6a)**—Starting from **4a** the compound was synthesized as described in procedure G (74%). The compound was also synthesized following procedure F. In this case 1/3 of methanol co-crystallized with **6a**, which could be removed by solving the crystals in water, removing some of the solvent under vacuum at 20 °C and freeze drying the resulting solution (91%): white crystals; mp = 232 °C;  $^1\text{H}$  NMR (DMSO- $d_6$ )  $\delta$  1.79–1.92 (m, 2H, 2CH), 2.06–2.12 (m, 2H, 2CH), 2.90–3.07 (m, 2H, 2CH),



3.15–3.28 (m, 3H, 3CH), 8.89–9.19 (m, 2H, NH<sub>2</sub>), 14.49 (s, 1H, NH); <sup>13</sup>C NMR (DMSO-d<sub>6</sub>) δ 24.96 (CH<sub>2</sub>), 30.50 (CH), 42.01 (CH<sub>2</sub>), 165.04 (Cq), 177.93 (Cq); EI-MS *m/z* 185 (M<sup>+</sup> free base). Anal. (C<sub>7</sub>H<sub>11</sub>N<sub>3</sub>OS·HCl) C, H, N, S.

**5-Piperidin-3-yl-3*H*-[1,3,4]oxadiazol-2-thione Hydrochloride. (6b)**—Starting from **4b** the compound was synthesized as described in procedure G, with the exception that 10% of the solvent were ethanol. The solvent was removed under reduced pressure and the residue recrystallized in ethanol: slightly green crystals (58%); mp = 219 °C; <sup>1</sup>H NMR (DMSO-d<sub>6</sub>) δ 1.70–1.85 (m, 3H, 3CH), 2.00–2.10 (m, 1H, CH), 2.80–2.92 (m, 1H, CH), 3.04–3.19 (m, 2H, 2CH), 3.34–3.43 (m, 2H, CH), 9.20–9.60 (m, 2H, NH<sub>2</sub>), 14.55 (s, 1H, NH); <sup>13</sup>C NMR (DMSO-d<sub>6</sub>) δ 20.75 (CH<sub>2</sub>), 24.88 (CH<sub>2</sub>), 30.82 (CH), 43.02 (CH<sub>2</sub>), 44.01 (CH<sub>2</sub>), 163.08 (Cq), 177.94 (Cq); EI-MS *m/z* 185 (M<sup>+</sup> free base). Anal. (C<sub>7</sub>H<sub>11</sub>N<sub>3</sub>OS·HCl·1/3H<sub>2</sub>O) C, H, N, S.

**L-5-Pyrrolidin-2-yl-3*H*-[1,3,4]oxadiazol-2-thione Hydrochloride. (6c)**—Starting from **4c** the compound was synthesized as described in procedure F: white crystals (50%); mp = 167 °C; <sup>1</sup>H NMR (DMSO-d<sub>6</sub>) δ 1.91–2.08 (m, 2H, 2CH), 2.15–2.36 (m, 2H, 2CH), 3.26 (app t, 6.44 Hz, 2H, 2CH), 4.80 (app t, 7.23 Hz, 2H, 2CH), 10.15 (s, 1H, NH); <sup>13</sup>C NMR (DMSO-d<sub>6</sub>) δ 23.79 (CH<sub>2</sub>), 27.73 (CH<sub>2</sub>), 45.71 (CH<sub>2</sub>), 52.13 (CH), 159.25 (Cq), 178.38 (Cq); EI-MS *m/z* 171 (M<sup>+</sup> free base); [α]<sub>D</sub><sup>20</sup> = -0.14 ° (RT, c = 0.58, H<sub>2</sub>O). Anal. (C<sub>6</sub>H<sub>9</sub>N<sub>3</sub>OS·HCl·1/3H<sub>2</sub>O) C, H, N, S.

**5-Aminomethyl-3*H*-[1,3,4]oxadiazol-2-thione Hydrochloride. (6d)**—Starting from **4d** the compound was synthesized as described in procedure F: beige crystals (71%); mp = 184 °C; <sup>1</sup>H NMR (DMSO-d<sub>6</sub>) δ 4.21 (s, 2H, CH<sub>2</sub>), 8.93 (s, 3H, NH<sub>3</sub>), 14.83 (s, 1H, NH); <sup>13</sup>C NMR (DMSO-d<sub>6</sub>) δ 33.56 (CH<sub>2</sub>), 158.27 (Cq), 178.21 (Cq); EI-MS *m/z* 131. Anal. (C<sub>3</sub>H<sub>5</sub>N<sub>3</sub>OS·HCl) C, H, N, S.

**5-Methylaminomethyl-3*H*-[1,3,4]oxadiazol-2-thione Hydrochloride. (6e)**—Starting from **4e** the compound was synthesized as described in procedure F: white crystals (81%); mp = 158 °C; <sup>1</sup>H NMR (DMSO-d<sub>6</sub>) δ 2.61 (s, 3H, CH<sub>3</sub>), 4.35 (s, 2H, CH<sub>2</sub>), 9.99 (s, 1H, NH); <sup>13</sup>C NMR (DMSO-d<sub>6</sub>) δ 32.96 (CH<sub>3</sub>), 41.51 (CH<sub>2</sub>), 156.95 (Cq), 178.22 (Cq); EI-MS *m/z* 145 (M<sup>+</sup>). Anal. (C<sub>4</sub>H<sub>7</sub>N<sub>3</sub>OS·HCl) C, H, N, S.

**[5-(2-Amino-ethyl)-3*H*-[1,3,4]oxadiazol-2-thione Hydrochloride. (6g)**—Starting from **4g** the compound was synthesized as described in procedure F: white crystals (94%); mp = 222 °C; <sup>1</sup>H NMR (DMSO-d<sub>6</sub>) δ 3.06–3.14 (m, 4H, CH<sub>2</sub>CH<sub>2</sub>), 8.26 (s, 3H, NH<sub>3</sub>), 14.48 (s, 1H, NH); <sup>13</sup>C NMR (DMSO-d<sub>6</sub>) δ 23.85 (CH<sub>2</sub>), 35.49 (CH<sub>2</sub>), 161.02 (Cq), 178.14 (Cq); EI-MS *m/z* 145 (M<sup>+</sup> free base). Anal. (C<sub>4</sub>H<sub>7</sub>N<sub>3</sub>OS·HCl) C, H, N.

#### General Procedures for the Synthesis of Oxadiazol-2-ones: Procedure H

**(Compounds 9a–c)**—The tertiary amine (2 equiv) was dissolved in CH<sub>2</sub>Cl<sub>2</sub> and cooled to 0 °C under a nitrogen atmosphere. After adding a solution of carbonic acid bis(trichloromethyl) carbonate (1 equiv) in CH<sub>2</sub>Cl<sub>2</sub> dropwise the mixture was refluxed. The reaction mixture was evaporated to dryness and the residue recrystallized or chromatographed (20–55%).

**5-(1-Methyl-piperidin-4-yl)-3*H*-[1,3,4]oxadiazol-2-one. (9a)**—Starting from **8a** the compound was synthesized as described in procedure H, and recrystallized from methanol: white crystals (55%); mp = 281 °C; <sup>1</sup>H NMR (DMSO-d<sub>6</sub>) δ 1.84–1.98 (m, 2H, 2CH), 2.05–2.15 (m, 2H, 2CH), 2.69 (s, 3H, CH<sub>3</sub>), 2.84–3.03 (m, 3H, 2CH), 3.14–3.44 (m, 2H, 2CH), 10.76 (s, 1H, NH), 12.25 (s, 1H, NH); EI-MS *m/z* 183 (M<sup>+</sup> free base). Anal. (C<sub>8</sub>H<sub>13</sub>N<sub>3</sub>O<sub>2</sub>·HCl·1/2H<sub>2</sub>O) C, H, N.

**5-(1-Benzyl-piperidin-4-yl)-3H-[1,3,4]oxadiazol-2-one Hydrochloride. (9b)—**

Starting from **8b** the compound was synthesized as described in procedure H, and recrystallized from methanol: white crystals (55%); mp = 253 °C; the NMR- and MS-data agreed with literature<sup>61</sup>. Anal. (C<sub>14</sub>H<sub>17</sub>N<sub>3</sub>O<sub>2</sub>·HCl) C, H, N.

**5-Dimethylaminomethyl-3H-[1,3,4]oxadiazol-2-one (9c)**—Starting from **8c** the compound was synthesized as described in procedure H. The mixture was poured onto water and extracted with ethyl acetate at pH 7. The combined organic extracts were dried (Na<sub>2</sub>SO<sub>4</sub>), the solvent was removed under vacuo and the residue chromatographed with ethyl acetate: white crystals (20%); mp = 103 °C; R<sub>f</sub> (ethyl acetate): 0.09; <sup>1</sup>H NMR (DMSO-d<sub>6</sub>) δ 2.18 (s, 6H, N(CH<sub>3</sub>)<sub>2</sub>), 3.36 (s, 2H, CH<sub>2</sub>), 12.22 (s, 1H, NH); <sup>13</sup>C NMR (DMSO-d<sub>6</sub>) δ 44.72 (2CH<sub>3</sub>), 53.52 (CH<sub>2</sub>), 154.76 (Cq), 155.27 (Cq); EI-MS *m/z* 143 (M<sup>+</sup>). Anal. (C<sub>5</sub>H<sub>9</sub>N<sub>3</sub>O<sub>2</sub>) C, H, N.

**5-Cyclohexyl-3H-[1,3,4]oxadiazole-2-one (9d)**—Starting from **8d** compound **9d** was prepared according to procedure H, and chromatographed: colorless oil which crystallizes on standing (85%); mp = 29 °C; IR data agreed with literature<sup>62</sup>; R<sub>f</sub> (petroleum ether/ethyl acetate = 2/1): 0.5; <sup>1</sup>H NMR (DMSO-d<sub>6</sub>) δ 1.13–1.43 (m, 5H, 5CH), 1.58–1.70 (m, 3H, 3CH), 1.85–1.88 (m, 2H, 2CH), 2.53–2.62 (m, 1H, CH), 12.03 (s, 1H, NH); <sup>13</sup>C NMR (DMSO-d<sub>6</sub>) δ 24.45 (2CH<sub>2</sub>), 25.07 (CH<sub>2</sub>), 28.45 (2CH<sub>2</sub>), 34.63 (CH), 154.89 (Cq), 159.71 (Cq); EI-MS *m/z* 168 (M<sup>+</sup>). Anal. (C<sub>8</sub>H<sub>12</sub>N<sub>2</sub>O<sub>2</sub>·1/5H<sub>2</sub>O) C, H, N.

**5-Methyl-3H-[1,3,4]oxadiazole-2-one (9e)**—Starting from **8e** compound **9e** was prepared according to procedure H, and recrystallized from CH<sub>2</sub>Cl<sub>2</sub> and n-hexane: white crystals (67%); mp = 112 °C<sup>63</sup>; <sup>13</sup>C-NMR-data agreed with literature<sup>50</sup>; <sup>1</sup>H NMR (DMSO-d<sub>6</sub>) δ 2.18 (s, 3H, CH<sub>3</sub>), 11.99 (s, 1H, NH); EI-MS *m/z* 101 (M<sup>+</sup>+1). Anal. (C<sub>3</sub>H<sub>4</sub>N<sub>2</sub>O<sub>2</sub>) C, H, N.

**5-(1-Methyl-piperidin-4-yl)-3H-[1,3,4]oxadiazole-2-thione (10a)**—A mixture of **8a** (1 equiv), pyridine (1.6 ml/equiv) and CS<sub>2</sub> (0.2 ml/equiv) was treated at 80–90 °C until the evolution of H<sub>2</sub>S had stopped. After removing the solvent under reduced pressure the residue was recrystallized in ethanol and subsequently in methanol. The compound was chromatographed and again recrystallized from methanol: beige crystals (17%); mp = 248 °C; R<sub>f</sub> (methanol): 0.5; <sup>1</sup>H NMR (DMSO-d<sub>6</sub>) δ 1.71–1.84 (m, 2H, 2CH), 2.00–2.10 (m, 2H, 2CH), 2.61 (s, 3H, CH<sub>3</sub>), 2.75–2.95 (m, 3H, 3CH), 3.18–3.27 (m, 2H, 2CH); <sup>13</sup>C NMR (DMSO-d<sub>6</sub>) δ 26.99 (2CH<sub>2</sub>), 30.54 (CH), 43.72 (CH<sub>3</sub>), 53.02 (2CH<sub>2</sub>), 164.41 (Cq), 178.93 (Cq); EI-MS *m/z* 199 (M<sup>+</sup>). Anal. (C<sub>8</sub>H<sub>13</sub>N<sub>3</sub>OS) C, H, N, S.

**5-(1-Benzyl-piperidin-4-yl)-3H-[1,3,4]oxadiazole-2-thione (10b)**—Was synthesized according to the synthesis described for compound **10a**, starting from **8b**: slightly beige crystals (34%); mp = 220 °C; R<sub>f</sub> (chloroform/methanol = 4/1): 0.4; the NMR- and MS-data agreed with literature<sup>61</sup>. Anal. (C<sub>14</sub>H<sub>17</sub>N<sub>3</sub>OS) C, H, N, S.

**5-Dimethylaminomethyl-3H-[1,3,4]oxadiazole-2-thione (10c)**—Starting from **8c** the compound was synthesized as described in procedure E. The mixture was poured onto water and extracted with ethyl acetate at pH 7. The combined organic extracts were dried (Na<sub>2</sub>SO<sub>4</sub>), the solvent was removed under vacuo and the residue chromatographed: beige crystals (5%); mp = 119 °C; R<sub>f</sub> (ethyl acetate): 0.08; <sup>1</sup>H NMR (DMSO-d<sub>6</sub>) δ 7.45 (d, 1H, IndH), 2.31 (s, 6H, N(CH<sub>3</sub>)<sub>2</sub>), 3.71 (s, 2H, CH<sub>2</sub>); <sup>13</sup>C NMR (DMSO-d<sub>6</sub>) δ 44.38 (CH<sub>3</sub>), 52.11 (CH<sub>2</sub>), 53.02 (2CH<sub>2</sub>), 160.35 (Cq), 178.80 (Cq); EI-MS *m/z* 159 (M<sup>+</sup>). Anal. (C<sub>5</sub>H<sub>9</sub>N<sub>3</sub>OS) C, H, N.

**5-Cyclohexyl-3H-[1,3,4]oxadiazole-2-thione (10d)**—Starting from **8d** compound **10d** was prepared according to procedure E, and chromatographed: slightly yellow crystals (46%); mp = 81 °C;  $R_f$  (petroleum ether/ethyl acetate = 5/1): 0.3;  $^1\text{H NMR}$  (DMSO- $d_6$ )  $\delta$  1.14–1.48 (m, 5H, 5CH), 1.57–1.71 (m, 3H, 3CH), 1.90–1.93 (m, 2H, 2CH), 2.74–2.84 (m, 1H, CH), 14.32 (s, 1H, NH);  $^{13}\text{C NMR}$  (DMSO- $d_6$ )  $\delta$  24.79 (2CH<sub>2</sub>), 25.34 (CH<sub>2</sub>), 29.05 (2CH<sub>2</sub>), 34.44 (CH), 167.10 (Cq), 177.87 (Cq); EI-MS  $m/z$  184 (M<sup>+</sup>). Anal. (C<sub>8</sub>H<sub>12</sub>N<sub>2</sub>OS) C, H, N.

**5-Methyl-3H-[1,3,4]oxadiazole-2-thione (10e)**—Starting from **8e** compound **10e** was prepared according to procedure E, and chromatographed: white crystals (17%); mp = 78 °C<sup>64</sup>;  $R_f$  (petroleum ether/ethyl acetate = 5/1): 0.1; NMR data agreed with literature<sup>65</sup>. EI-MS  $m/z$  117 (M<sup>+</sup>+1). Anal. (C<sub>3</sub>H<sub>4</sub>N<sub>2</sub>OS) C, H, N.

#### General Procedures for the Synthesis of [1,3,4]Oxadiazols: Procedure I

**(Compounds 11, 18)**—The hydrazide was refluxed for two hours in excess triethoxyalkane. Afterwards alcohol which is formed during the reaction was removed by distillation. The residue was refluxed for 5 hours. After cooling to RT, the mixture was treated with water, saturated with K<sub>2</sub>CO<sub>3</sub> and extracted several times with ethyl acetate. The combined organic extracts were dried (Na<sub>2</sub>SO<sub>4</sub>), evaporated and chromatographed (62–66%).

**1-Be nzyI-4-[1,3,4]oxadiazol-2-yl-piperidine. (11)**—Starting from **8b** and triethoxyethane the compound was prepared according to procedure I, and chromatographed starting with petroleum ether/ethyl acetate = 1/1 and switching to methanol/ethyl acetate = 1/1: white slightly beige crystals (62%); mp = 61 °C;  $R_f$  (ethyl acetate/petroleum ether = 1/1): 0.1;  $R_f$  (methanol/ethyl acetate = 1/1): 0.4;  $^1\text{H NMR}$  (DMSO- $d_6$ )  $\delta$  1.64–1.77 (m, 2H, 2CH), 1.90–2.00 (m, 2H, 2CH), 2.03–2.11 (m, 2H, 2CH), 2.74–2.84 (m, 2H, 2CH), 2.89–2.99 (m, 1H, CH), 3.45 (s, 2H, CH<sub>2</sub>-Ph), 7.18–7.32 (m, 5H, CH<sub>Ar</sub>), 9.13 (s, 1H, CH<sub>Oxadiazole</sub>);  $^{13}\text{C NMR}$  (DMSO- $d_6$ )  $\delta$  29.32 (2CH<sub>2</sub>), 32.55 (CH), 52.31 (2CH<sub>2</sub>), 62.56 (CH<sub>2</sub>), 127.17 (CH), 128.45 (2CH), 129.05 (2CH), 138.63 (Cq), 154.46 (CH), 168.67; EI-MS  $m/z$  244 (M<sup>+</sup>). Anal. (C<sub>14</sub>H<sub>17</sub>N<sub>3</sub>O) C, H, N.

**4-Benzyl-5-piperidin-4-yl-2,4-dihydro-[1,2,4]triazol-3-one Hydrochloride. (16a)**—Starting from **14a** compound **16a** was synthesized as described in procedure F: white crystals (66%); mp = 251 °C;  $^1\text{H NMR}$  (DMSO- $d_6$ )  $\delta$  1.65–1.80 (m, 4H, 4CH), 2.77–2.95 (m, 3H, 3CH), 3.15–3.25 (m, 2H, 2CH), 4.81 (s, 2H, CH<sub>2</sub>-Ph), 7.21–7.37 (m, 5H, CH<sub>Ar</sub>), 8.85–9.25 (m, 2H, NH<sub>2</sub>), 11.70 (s, 1H, NH);  $^{13}\text{C NMR}$  (DMSO- $d_6$ )  $\delta$  26.29 (2CH<sub>2</sub>), 30.21 (CH), 42.48 (2CH<sub>2</sub>), 43.36 (CH<sub>2</sub>), 78.44 (Cq), 127.19 (2CH), 127.89 (CH), 129.03 (2CH), 137.31 (Cq), 149.47 (Cq), 155.30 (Cq); EI-MS  $m/z$  258 (M<sup>+</sup>). Anal. (C<sub>13</sub>H<sub>19</sub>N<sub>4</sub>O·HCl·5/4H<sub>2</sub>O) C, H, N.

**5-Aminomethyl-4-benzyl-2,4-dihydro-[1,2,4]triazol-3-one. (16d)**—Starting from **12d** compound **16a** was synthesized as described in procedure L, since no precipitate was formed the mixture was extracted with several portions of ethyl acetate. The combined organic extracts were dried (Na<sub>2</sub>SO<sub>4</sub>) and the solvent evaporated under vacuo until the crystallization started: white crystals (44%); mp = 150 °C;  $^1\text{H NMR}$  (DMSO- $d_6$ )  $\delta$  1.78 (s, 2H, NH<sub>2</sub>), 3.44 (s, 2H, CH<sub>2</sub>N), 4.86 (s, 2H, CH<sub>2</sub>-Ph), 7.22–7.37 (m, 5H, CH<sub>Ar</sub>), 11.55 (s, 1H, NH);  $^{13}\text{C NMR}$  (DMSO- $d_6$ )  $\delta$  37.76 (CH<sub>2</sub>), 43.30 (CH<sub>2</sub>), 127.35 (2CH), 127.80 (CH), 128.96 (2CH), 137.38 (Cq), 148.79 (Cq), 155.73 (Cq); EI-MS  $m/z$  204 (M<sup>+</sup>). Anal. (C<sub>10</sub>H<sub>12</sub>N<sub>4</sub>O) C, H, N.

**4-Benzyl-5-piperidin-4-yl-2,4-dihydro-[1,2,4]triazol-3-thione Hydrochloride. (17a)**—Starting from **15** compound **17a** was synthesized as described in procedure F: white crystals (95%); mp = 285 °C;  $^1\text{H NMR}$  (DMSO- $d_6$ )  $\delta$  1.63–1.78 (m, 4H, 4CH), 2.79–2.91 (m, 2H, 2CH), 2.98–3.08 (m, 1H, CH), 3.14–3.22 (m, 2H, 2CH), 5.27 (s, 2H, CH<sub>2</sub>-Ph), 7.26–7.37 (m, 5H, CH<sub>Ar</sub>), 8.68–9.04 (m, 2H, NH<sub>2</sub>), 13.83 (s, 1H, NH);  $^{13}\text{C NMR}$  (DMSO- $d_6$ )  $\delta$  26.64

(2CH<sub>2</sub>), 30.31 (CH), 42.49 (2CH<sub>2</sub>), 45.91 (CH<sub>2</sub>), 127.36 (2CH), 128.12 (CH), 129.03 (2CH), 136.29 (Cq), 154.60 (Cq), 167.43 (Cq); EI-MS *m/z* 274 (M<sup>+</sup>). Anal. (C<sub>14</sub>H<sub>18</sub>N<sub>4</sub>S·HCl·5/4H<sub>2</sub>O) C, H, N, S.

**5-Aminomethyl-4-benzyl-2,4-dihydro-[1,2,4]triazol-3-thione. (17d)**—Starting from **13d** compound **17d** was synthesized as described in procedure L, and chromatographed with petroleum ether/ethyl acetate = 1/3 to wash off most of the intermediate BOC-protected triazole-3-thione, and then with ethyl acetate/methanol = 1/5, and subsequently with CHCl<sub>3</sub>/methanol = 4/1: white crystals (11%); mp = 69 °C; R<sub>f</sub> (CHCl<sub>3</sub>/methanol = 4/1): 0.52; white crystals (11%); mp = 158 °C; <sup>1</sup>H NMR (DMSO-d<sub>6</sub>) δ 2.07 (s, 2H, NH<sub>2</sub>), 3.15 (s, 1H, NH), 3.55 (s, 2H, CH<sub>2</sub>NH<sub>2</sub>), 5.32 (s, 2H, CH<sub>2</sub>-Ph), 7.26–7.39 (m, 5H, CH<sub>Ar</sub>); <sup>13</sup>C NMR (DMSO-d<sub>6</sub>) δ 37.23 (CH<sub>2</sub>), 45.71 (CH<sub>2</sub>), 127.39 (2CH), 128.02 (CH), 128.98 (2CH), 136.24 (Cq), 153.74 (Cq), 167.89 (Cq); EI-MS *m/z* 220 (M<sup>+</sup>). Anal. (C<sub>10</sub>H<sub>12</sub>N<sub>4</sub>S·9/10H<sub>2</sub>O) C, H, N, S.

**4-(5-Methyl-[1,3,4]oxadiazol-2-yl)-piperidine Hydrochloride. (19)**—Starting from **18** the compound was synthesized as described in general procedure G (56%); the corresponding hydrobromide was obtained by stirring 2.6 mmol of **18** in 1 mL of HBr in Acetic Acid (5.7 M) under a nitrogen atmosphere overnight (98%). Analytical data for the hydrochloride: mp = 193 °C; <sup>1</sup>H NMR (DMSO-d<sub>6</sub>) δ 1.85–1.99 (m, 2H, 2CH), 2.09–2.14 (m, 2H, 2CH), 2.45 (s, 3H, CH<sub>3</sub>), 2.94–3.05 (m, 2H, 2CH), 3.22–3.33 (m, 3H, 3CH), 9.11–9.35 (m, 2H, NH<sub>2</sub>); <sup>13</sup>C NMR (DMSO-d<sub>6</sub>) δ 10.80 (CH<sub>3</sub>), 25.66 (2CH<sub>2</sub>), 30.24 (CH), 42.13 (2CH<sub>2</sub>), 163.98 (Cq), 167.68 (Cq). Anal. (C<sub>8</sub>H<sub>13</sub>N<sub>3</sub>O·HCl·5/3H<sub>2</sub>O) C, H, N.

**[<sup>3</sup>H]Muscimol Ligand binding assays**—Adult, male Sprague-Dawley rats (supplied by the Department of Laboratory Animals, University of Mainz) were decapitated, their brains removed and cerebellum and cortex separated. The tissue was homogenized in 50 mM Tris/citrate, pH 7.3, in an Ultraturrax (IKA, Staufen, Germany) for 15 sec. The membranes were centrifuged at 43,000 ×g for 20 min. The washing step was repeated four times before the membranes were frozen at –20 °C. After slow thawing the washing steps were repeated another two times and frozen again until use. Before each experiment the membranes were recentrifuged and diluted to the desired protein concentration. Resuspended cell membranes (50–200 μg protein per tube) were incubated in a final volume of 0.5 ml of 50 mM Tris/citrate buffer, pH 7.3, for [<sup>3</sup>H]muscimol binding (6 nM) with and without the novel compounds in the concentration range given in the text. Non-specific binding was determined in the presence of 100 μM GABA. After 60 min on ice the assay mixtures were rapidly diluted to 5 ml with ice-cold 10 mM Tris/HCl, pH 7.4, filtered through glass fiber filters (# 52, Schleicher & Schuell, Dassel, Germany) and washed once with 5 ml 10 mM Tris/HCl, pH 7.4. Filters were immersed in 4 ml of Zinsser AquaSolv (Munich, Germany) scintillation fluid, and the radioactivity determined in a Beckman liquid scintillation counter using external standardization. Statistical calculations were performed using the Graph Pad Prism program (GraphPad Software, San Diego, CA.) with and without the novel compounds.

**Cell culturing and cell transfection**—For electrophysiological recording, HEK-293 cells were passaged and replated on 12-mm glass coverslips located in 9.6-cm plastic dishes filled with 10 ml of Minimum Essential Medium (MEM, Gibco) supplemented with 158 mg/l sodium bicarbonate, 2 mM glutamine (Gibco), 100 U/ml penicillin-streptomycin (Gibco), and 10% fetal calf serum (Gibco). Cultures were maintained at 37 °C in a humidified 95% O<sub>2</sub>/5% CO<sub>2</sub> atmosphere for 2–3 days.

Transfection with recombinant rat GABA<sub>A</sub> receptors were carried out as described in detail<sup>66, 67</sup>. Briefly, HEK 293 cells were transfected using the calcium phosphate precipitation method with rat GABA<sub>A</sub> receptor cDNAs in eukaryotic expression vectors<sup>68</sup> for the α, β and

$\gamma$  subunits. For optimal receptor expression, final concentrations ( $\mu\text{g}$  vector DNA per 9.6 cm tissue culture plate) were:  $\alpha_1$ , 2;  $\alpha_2$  4.8;  $\alpha_3$ , 1.2;  $\alpha_4$  10;  $\alpha_5$ , 0.8;  $\alpha_6$ , 2;  $\beta_3$ , 0.4; and  $\gamma_2\text{S}$ , 0.3. The  $\gamma_2\text{S}$  variant is abbreviated  $\gamma_2$  in the remainder of the text. To identify transfected cells all subunit combinations were co-transfected with 1  $\mu\text{g}$  per plate of pNI-EGFP.

**HEK293 Electrophysiology**—Two days after transfection single coverslips containing HEK 293 cells were placed in a recording chamber mounted on the movable stage of a fluorescence microscope (Olympus IX70) and perfused with a defined saline solution containing (in mM): 130 NaCl, 5.4 KCl, 2 CaCl<sub>2</sub>, 2 MgSO<sub>4</sub>, 10 glucose, 5 sucrose, and 10 HEPES (free acid), pH adjusted to 7.35 with NaOH. Transfected cells were identified by their green fluorescence due to the expression of the pNI-EGFP vector. Ligand-mediated membrane currents from these cells were studied using the whole-cell patch-clamp recording technique<sup>69</sup>. Patch pipettes were pulled from hard borosilicate capillary glass (0.5 mm ID, 1.5 mm OD, Vitrex, Science Products GmbH, Hofheim, Germany) using a horizontal puller (Sutter Instruments, CA, Model P-97) in a multi-stage process. The pipettes had an initial resistance of 2–4 M $\Omega$  when filled with a solution containing (in mM): 90 KCl, 50 KOH, 2 CaCl<sub>2</sub>, 2 MgCl<sub>2</sub>, 10 EGTA, 3.1 ATP (di-potassium salt), 0.4 GTP (tri-sodium salt), and 10 HEPES (free acid), pH 7.35.

The junction potential between the pipette and the external solution was less than 2.3 mV and therefore was neglected. Seal resistances >1 G $\Omega$  were routinely obtained by applying gentle suction to the pipettes. Membrane rupture was monitored electrically as an increase in capacitance. Pipette capacitance, membrane capacitance, and series resistance were electronically compensated to minimize capacitive transients. A series resistance compensation of > 60% was regularly used.

To analyze modulations of the GABA-induced currents the approximate receptor subtype specific GABA EC<sub>20</sub> and increasing drug concentrations were applied to the cells using a fast perfusion stepper system (SF-77B, Perfusion Fast Step, Warner Instruments, Inc., Midwest, USA). In the case of **5a** and **6a** the following concentrations were co-applied (in  $\mu\text{M}$ ): 0.1, 1, 10, 100, 1000, for **19** and **5d** the concentration range used was (in M): 0.1, 0.3, 1, 3, 10, 30, 100, 300, 1000. Additionally the intrinsic activity of all compounds was tested by applying them alone to the cells in concentrations of 1, 10, 100, and 1000  $\mu\text{M}$ .

Responses of cells were recorded by patch-clamp amplifier (EPC-8, HEKA-Electronic, Lambrecht, Germany) in conjunction with a standard personal computer and the pClamp 8.1 software package (Axon Instruments, Foster City, CA). The standard holding-potential for the cells was  $-40$  mV. Whole cell currents were low-pass filtered by a eight-pole Bessel filter at 5 or 3 kHz before being digitized by a Digidata 1322A interface (Axon Instruments, Foster City, CA) and recorded by the computer at a sampling rate of at least 5 kHz.

**Mutagenesis and oocyte expression**—The rat GABA<sub>A</sub> receptor  $\alpha_1$  and  $\beta_2$  subunit DNA constructs in the pGH19 vector ( $\alpha_1$  wild-type (wt),  $\alpha_1\text{F64C}$ ,  $\alpha_1\text{R66C}$ ,  $\alpha_1\text{S68C}$ ,  $\alpha_1\text{T129C}$ ,  $\beta_2$  wt) were obtained from Dr. Cynthia Czajkowski, University of Wisconsin-Madison. Their identity was verified by restriction digestion and DNA sequencing. Plasmids were linearized with NheI prior to *in vitro* mRNA transcription with T7 RNA polymerase (Amplicap T7 High Yield Message Maker<sup>TM</sup>, Epicentre Technologies, Madison, WI). mRNA was dissolved in diethylpyrocarbamate-treated water, and stored at  $-80$  °C. Female *Xenopus laevis* were purchased from Nasco Science (Fort Atkinson, WI). Stage V-VI oocytes were defolliculated with a 75 minute treatment with 2 mg/ml Type 1A collagenase (Sigma Chemical Co., St. Louis, MO) in OR2 (82.5 mM NaCl, 2 mM KCl, 1 mM MgCl<sub>2</sub>, and 5 mM HEPES; pH adjusted to 7.5 with NaOH). Oocytes were washed thoroughly in OR2 and kept in SOS medium (82.5 mM NaCl, 2.5 mM KCl, 1 mM MgCl<sub>2</sub>, 5 mM HEPES, pH 7.5) supplemented with 1% Antibiotic-



Antimycotic (100X) liquid (10,000 IU/ml penicillin, 10,000 µg/ml streptomycin, and 25 µg/ml of amphotericin B; Invitrogen, Carlsbad, CA) and 5% horse serum (Sigma). Oocytes were injected 24 h after isolation with 50 nl (10 ng) of a 1:1 mixture of rat  $\alpha_1:\beta_2$  subunit mRNA and were kept in horse serum medium for 2 to 10 days at 17 °C. Mutant subunit mRNA was substituted for wt  $\alpha_1$  subunit where necessary<sup>70</sup>.

**Two electrode voltage clamp recording**—The electrophysiological recordings were conducted at room temperature in a ~250-µl chamber continuously perfused at a rate of 5 to 6 ml/min with Ca<sup>2+</sup>-free frog Ringer buffer (CFFR; 115 mM NaCl, 2.5 mM KCl, 1.8 mM MgCl<sub>2</sub>, 10 mM HEPES pH 7.5 with NaOH) using equipment and procedures described previously<sup>52</sup>. Currents were recorded from individual oocytes using two-electrode voltage-clamp at a holding potential of -60 mV. The ground electrode was connected to the bath via a 3 M KCl/Agar bridge. Glass microelectrodes had a resistance of < 2 MΩ when filled with 3 M KCl. Data were acquired and analyzed using a TEV-200 amplifier (Dagan Instruments, Minneapolis, MN), a Digidata 1200 or Digidata 1322A data interface (Axon Instruments, Union City, CA), and pClamp 7 or pClamp 8 software (Axon Instruments). Currents ( $I_{\text{GABA}}$ ) were elicited by applications of GABA separated by at least 5 min of CFFR wash to allow complete recovery from desensitization. Currents were judged to be stable if the variation between consecutive GABA pulses was <10%.

**Reagents**—The sulfhydryl-reactive methanethiosulfonate (MTS) reagents used in these experiments were 2-sulfonatoethyl methanethiosulfonate (MTSES<sup>-</sup>) and 2-((biotinoyl)amino)ethyl methanethiosulfonate (MTSEA-biotin) (Biotium, Inc., Hayward, CA). MTS-reagents react with cysteine (Cys) and covalently couple a 2-sulfonatoethylsulfide (MTSES<sup>-</sup>) or a 2-((biotinoyl)amino)ethylsulfide moiety (MTSEA-biotin) onto protein sulfhydryls. A 100 mM stock solution of MTSES<sup>-</sup> in water or MTSEA-biotin in DMSO was prepared daily and kept on ice. The working solutions were obtained by diluting the 100 mM stock solution in CFFR immediately before use. GABA (Sigma) was prepared as a 100 mM stock solution in water. Dithiothreitol (DTT) (Sigma) was dissolved in water to obtain a 1 M stock solution and diluted into CFFR before each experiment.

**GABA and 6a Concentration-Response Relationships**—The GABA EC<sub>50</sub>s for wt or mutant  $\alpha_1\beta_2$  receptors were determined using the two-electrode voltage clamp technique on *Xenopus laevis* oocytes. To determine the GABA concentration-response relationship, progressively increasing GABA concentrations were applied to oocytes expressing wt or mutant receptors. The currents were normalized to the maximal GABA-induced current ( $I_{\text{max}}$ ). The GABA concentration-response relationship was determined for each mutant by least-squares minimization (GraphPad Prism 3.0, GraphPad Software Inc., San Diego, CA; SigmaPlot 2000, SPSS Inc., Chicago, IL) of the currents to a logistic equation of the form:

$$I/I_{\text{max}} = 1/(1 + (\text{EC}_{50}/[\text{GABA}])^n)$$

where  $n$  is the Hill coefficient and EC<sub>50</sub> is the GABA concentration that gives rise to 50% of the maximal current. Parameters from several oocytes were averaged to obtain the mean EC<sub>50</sub> and Hill coefficient. Data are presented as mean ± S.E.M. except where the number of experiments performed is two in which case average errors are given.

For  $\alpha_1\beta_2$  wt,  $\alpha_1\text{F64C}\beta_2$ , and  $\alpha_1\text{S68C}\beta_2$  receptors we also performed concentration-response experiments with **6a** - which directly activates at high concentrations - to measure the EC<sub>50</sub> for this compound. For **6a** dose-response curves only two trials were performed for some mutants due to the limited supply of **6a**.

**Determination of 6a IC<sub>50</sub>**—The IC<sub>50</sub> for **6a** was determined by co-applying progressively increasing test concentrations of **6a** with a constant GABA concentration. For each receptor

the GABA EC<sub>20</sub> concentration was used. We used a low GABA concentration for our inhibition experiments because of the limited availability of **6a**. Inhibition was calculated as  $I_{\text{GABA} + \mathbf{6a}}/I_{\text{GABA}}$ . Data were fit to the following equation:

$$\text{inhibition} = 1 - 1/(1 + (\text{IC}_{50}/[\mathbf{6a}])^n)$$

where IC<sub>50</sub> is the concentration of **6a** that blocks half of I<sub>GABA</sub>; [**6a**] is the concentration of **6a**, and *n* is the Hill coefficient.

**Picrotoxinin blockade of 6a induced currents**—We applied several **6a** (10 mM) test-pulses to α<sub>1</sub>β<sub>2</sub> receptors and recorded the induced currents. Following wash-out we applied the open-channel blocker picrotoxinin (100 μM) immediately followed by a co-application of **6a** and picrotoxinin (10 mM and 100 μM) and recorded the current trace.

**Determination of MTS-reagent reaction rates**—The MTS reagent was applied repeatedly in the extracellular bath for brief periods. Before and between each application of MTS reagent, the GABA-induced current was determined. For each mutant, the MTS-reagent concentration to be used was chosen based on preliminary experiments so that the reaction would proceed to completion in 1 to 2 min of cumulative MTS-reagent application time (MTSES<sup>−</sup> concentrations used: α<sub>1</sub>F64C, 10 μM; α<sub>1</sub>R66C, 250 and 500 μM; α<sub>1</sub>S68C, 150 μM; α<sub>1</sub>T129C, 10 nM; MTSEA-biotin concentration used: α<sub>1</sub>R66C, 10 or 40 μM; α<sub>1</sub>T129C, 10 nM). The peak GABA test currents were normalized to the initial GABA current, plotted as a function of the cumulative MTS-reagent application time and fitted with a monoexponential function of the form,

$$I = (I_0 - I_\infty)e^{-t\tau'} + I_\infty$$

where I<sub>0</sub> is the value of the GABA-induced current amplitude before modification, I<sub>∞</sub> is the current amplitude at the end of the reaction, *t* is the cumulative MTS-reagent application time, and τ' is the pseudo-first-order rate constant (s<sup>−1</sup>). The second-order rate constants, τ, were calculated by dividing the pseudo-first-order time constants τ' by the MTS-reagent concentration. The second-order rate constants were independent of the MTS-reagent concentrations used. MTS-reagent reaction rates were determined for α<sub>1</sub>F64C, α<sub>1</sub>R66C, as well as α<sub>1</sub>S68C containing α<sub>1</sub>β<sub>2</sub> GABA<sub>A</sub> receptors. Data are presented as mean ± S.E.M. These rates were used to calculate the concentration and time of application of MTS-reagent that produces submaximal, non-saturating inhibition.

**Determination of 6a reaction rates in α<sub>1</sub>R66Cβ<sub>2</sub> receptors**—**6a** was applied repeatedly in the extracellular bath for brief periods. Before and between each **6a** application the GABA-induced current was determined. The **6a** reaction rate with the engineered α<sub>1</sub>R66C was determined as described above for MTS-reagents. Once the alternating **6a** and GABA applications produced a reduced but stable GABA current we applied a saturating amount of MTSES<sup>−</sup> (10 mM, 12 s) in order to determine whether all of the engineered cysteines had reacted with **6a**. In order to demonstrate that the **6a** inhibition of α<sub>1</sub>R66C was due to formation of a disulfide bond between **6a** and the engineered cysteine thiol we applied DTT (10 mM, 20 s), and measured the GABA current again.

**Protection assay with 6a or GABA in mutant α<sub>1</sub>β<sub>2</sub> receptors**—In order to demonstrate that **6a** or GABA bound in close proximity to an engineered cysteine we assayed the ability of these agonists to protect the cysteine from reaction with an MTS reagent. In order to maximize our ability to detect protection we used concentrations of MTS reagents and durations of application that caused large but sub-maximal inhibition of the subsequent GABA test currents. For a 12-sond application, the MTSES<sup>−</sup> concentrations used were: α<sub>1</sub>F64C, 10

$\mu\text{M}$ ;  $\alpha_1\text{R66C}$ , 2 mM;  $\alpha_1\text{S68C}$ , 450  $\mu\text{M}$ ; and MTSEA-biotin concentration:  $\alpha_1\text{R66C}$ , 30  $\mu\text{M}$ . To detect protection for a given mutant, an initial GABA test current was determined. We co-applied a concentration-duration of MTS-reagent that produced sub-maximal inhibition together with **6a** (10 or 30 mM) or GABA  $\text{EC}_{90}$  concentrations. After washout the remaining GABA-induced current was determined. In order to determine the percent inhibition caused by the MTS + **6a** or GABA co-application it was important to determine the maximum extent of inhibition for each oocyte. This was determined by a subsequent application of a saturating amount of MTS reagent (MTSES<sup>-</sup> concentration:  $\alpha_1\text{F64C}$ , 20  $\mu\text{M}$ , 50 s;  $\alpha_1\text{R66C}$ , 10 mM, 12 s;  $\alpha_1\text{S68C}$ , 5 mM, 12 s; MTSEA-biotin concentration:  $\alpha_1\text{R66C}$ , 300  $\mu\text{M}$ , 12 s) followed by a determination of the current induced by a subsequent GABA-test pulse. If the extent of inhibition resulting from co-application of the MTS reagent with **6a** or GABA was less than the extent of inhibition when just the MTS reagent was applied then we inferred that **6a** and/or GABA had protected the cysteine from modification by the MTS reagent.

The amount of reaction was calculated using the equation:

$$\% \text{ reduction} = (I_0 - I) / (I_0 - I_\infty) \times 100$$

where  $I_0$  is the value of the GABA-induced current amplitude before modification,  $I$  is the current amplitude after application of the concentration and duration of MTS-reagent that produced sub-maximal inhibition with or without ligand (GABA or **6a**), and  $I_\infty$  is the current amplitude at the end of the reaction after maximal inhibition. Note that the MTS-reagent rates of reaction were done by applying the reagents via a continuous perfusion system. In the protection assay we used a syringe application system that allowed us to use small volumes because of the limited availability of **6a**.

**Homology modeling**—The extracellular domains of rat GABA<sub>A</sub> receptor  $\alpha_1$  and  $\beta_2$  subunits were modeled on the basis of the 2.2 Å crystal structure of the homologous homopentameric Acetylcholine-Binding Protein (AChBP) with nicotine bound (PDB # 1UW6). Using Deep View/Swiss Pdb-Viewer v3.7<sup>71</sup> we aligned the  $\alpha_1$  and  $\beta_2$  subunit sequences with the AChBP A and E chain, respectively<sup>57</sup>. The AChBP structure aligned with the raw sequence was submitted as a modeling request in Swiss Model. The resulting homology modeled  $\alpha_1\beta_2$  structure was subsequently subjected to energy minimization and later rendered with POV-Ray v3.6 (<http://www.povray.org/>)<sup>72</sup>.

## Supplementary Material

Refer to Web version on PubMed Central for supplementary material.

## Acknowledgements

We thank Dr. Cindy Czajkowski (Univ. of Wisconsin-Madison) for the generous gift of the GABA<sub>A</sub> receptor  $\alpha_1$  subunit cysteine-substitution mutants. We thank Rachel Berkowitz (Albert Einstein College of Medicine), Monique Jakob, Johanna Jambor, Matthias Platz (Univ. of Mainz) for technical assistance and Moez Bali, Amal Bera, Jeffrey Horenstein, David Liebelt and David Reeves (Albert Einstein College of Medicine) for helpful discussions and also for comments on this manuscript. We thank Angela Bauer, Inna Giesbrecht, Werner Kiefer, Angelika Krauß, Christian Peifer and Philip Prech (Univ. of Mainz) for helpful discussions on the synthesis. Supported in part by grants from the National Institutes of Health NS030808 and GM077660 (to MHA) and by K99NS059841 (to MJ) and by a Deutsche Forschungsgemeinschaft fellowship to MJ (JA-1081/1). Financial support by the Deutsche Forschungsgemeinschaft (HL), 'Fonds der Chemischen Industrie' (HL, HR) is gratefully acknowledged.

## Abbreviations

**ACh**  
acetylcholine

<b>AChBP</b>	acetylcholine binding protein
<b>DTT</b>	dithiothreitol
<b>GABA</b>	$\gamma$ -aminobutyric acid
<b>GABA<sub>A</sub></b>	GABA Type A receptors
<b>MTS</b>	methanethiosulfonate
<b>MTSES<sup>-</sup></b>	methanethiosulfonate ethylsulfonate
<b>SCAM</b>	substituted cysteine accessibility method

## References

1. Barnard EA, Skolnick P, Olsen RW, Mohler H, Sieghart W, Biggio G, Braestrup C, Bateson AN, Langer SZ. International Union of Pharmacology. XV. Subtypes of gamma-aminobutyric acidA receptors: classification on the basis of subunit structure and receptor function. *Pharmacol Rev* 1998;50(2):291–313. [PubMed: 9647870]
2. Bonnert TP, McKernan RM, Farrar S, le Bourdelles B, Heavens RP, Smith DW, Hewson L, Rigby MR, Sirinathsinghi DJ, Brown N, Wafford KA, Whiting PJ. theta, a novel gamma-aminobutyric acid type A receptor subunit. *Proc Natl Acad Sci U S A* 1999;96(17):9891–6. [PubMed: 10449790]
3. Sinkkonen ST, Hanna MC, Kirkness EF, Korpi ER. GABA(A) receptor epsilon and theta subunits display unusual structural variation between species and are enriched in the rat locus ceruleus. *J Neurosci* 2000;20(10):3588–95. [PubMed: 10804200]
4. Böhme I, Rabe H, Lüddens H. Four amino acids in the alpha subunits determine the gamma-aminobutyric acid sensitivities of GABAA receptor subtypes. *J Biol Chem* 2004;279(34):35193–200. [PubMed: 15199051]
5. Sieghart W, Sperk G. Subunit composition, distribution and function of GABA(A) receptor subtypes. *Curr Top Med Chem* 2002;2(8):795–816. [PubMed: 12171572]
6. Nusser Z, Sieghart W, Somogyi P. Segregation of different GABA<sub>A</sub> receptors to synaptic and extrasynaptic membranes of cerebellar granule cells. *J Neurosci* 1998;18(5):1693–703. [PubMed: 9464994]
7. Fritschy JM, Johnson DK, Mohler H, Rudolph U. Independent assembly and subcellular targeting of GABA(A)-receptor subtypes demonstrated in mouse hippocampal and olfactory neurons in vivo. *Neurosci Lett* 1998;249(2–3):99–102. [PubMed: 9682826]
8. Lüddens H, Korpi ER. Biological function of GABAA/benzodiazepine receptor heterogeneity. *J Psychiatr Res* 1995;29(2):77–94. [PubMed: 7545236]
9. Quirk K, Blurton P, Fletcher S, Leeson P, Tang F, Mellilo D, Ragan CI, McKernan RM. [3H]L-655,708, a novel ligand selective for the benzodiazepine site of GABAA receptors which contain the alpha 5 subunit. *Neuropharmacology* 1996;35(9–10):1331–5. [PubMed: 9014149]
10. Skolnick P, Hu RJ, Cook CM, Hurt SD, Trometer JD, Liu R, Huang Q, Cook JM. [3H]RY 80: A high-affinity, selective ligand for gamma-aminobutyric acidA receptors containing alpha-5 subunits. *J Pharmacol Exp Ther* 1997;283(2):488–93. [PubMed: 9353361]
11. Lüddens H, Pritchett DB, Kohler M, Killisch I, Keinänen K, Monyer H, Sprengel R, Seeburg PH. Cerebellar GABAA receptor selective for a behavioural alcohol antagonist. *Nature* 1990;346(6285):648–51. [PubMed: 2166916]

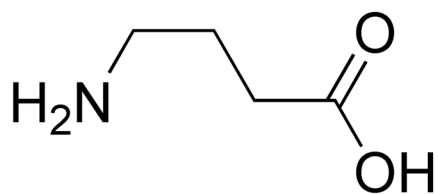
12. Wisden W, Seeburg PH. GABA<sub>A</sub> receptor channels: from subunits to functional entities. *Current Opinions in Neurobiology* 1992;2:263–269.
13. Pritchett DB, Sontheimer H, Shivers BD, Ymer S, Kettenmann H, Schofield PR, Seeburg PH. Importance of a novel GABA<sub>A</sub> receptor subunit for benzodiazepine pharmacology. *Nature* 1989;338:582–585. [PubMed: 2538761]
14. Sigel E, Buhr A. The benzodiazepine binding site of GABA<sub>A</sub> receptors. *Trends Pharmacol Sci* 1997;18(11):425–9. [PubMed: 9426470]
15. Saarelainen KS, Ranna M, Rabe H, Sinkkonen ST, Moykkynen T, Uusi-Oukari M, Linden AM, Luddens H, Korpi ER. Enhanced behavioral sensitivity to the competitive GABA agonist, gaboxadol, in transgenic mice over-expressing hippocampal extrasynaptic alpha6beta GABA(A) receptors. *J Neurochem.* 2007
16. Korpi ER, Luddens H. Furosemide interactions with brain GABAA receptors. *Br J Pharmacol* 1997;120(5):741–8. [PubMed: 9138676]
17. Korpi ER, Kuner T, Seeburg PH, Luddens H. Selective antagonist for the cerebellar granule cell-specific gamma-aminobutyric acid type A receptor. *Mol Pharmacol* 1995;47(2):283–9. [PubMed: 7870036]
18. Korpi ER, Wong G, Luddens H. Subtype specificity of gamma-aminobutyric acid type A receptor antagonism by clozapine. *Naunyn Schmiedebergs Arch Pharmacol* 1995;352(4):365–73. [PubMed: 8532064]
19. Barbee JG. Memory, benzodiazepines, and anxiety: integration of theoretical and clinical perspectives. *J Clin Psychiatry* 1993;54(Suppl):86–97. [PubMed: 8262893]discussion 98–101
20. Salinas JA, McGaugh JL. Muscimol induces retrograde amnesia for changes in reward magnitude. *Neurobiol Learn Mem* 1995;63(3):277–85. [PubMed: 7670841]
21. Huang Q, Liu R, Zhang P, He X, McKernan R, Gan T, Bennett DW, Cook JM. Predictive models for GABAA/benzodiazepine receptor subtypes: studies of quantitative structure-activity relationships for imidazobenzodiazepines at five recombinant GABAA/benzodiazepine receptor subtypes [alphaXbeta3gamma2 (x = 1–3, 5, and 6)] via comparative molecular field analysis. *J Med Chem* 1998;41(21):4130–42. [PubMed: 9767648]
22. Huang Q, He X, Ma C, Liu R, Yu S, Dayer CA, Wenger GR, McKernan R, Cook JM. Pharmacophore/receptor models for GABA(A)/BzR subtypes (alpha1beta3gamma2, alpha5beta3gamma2, and alpha6beta3gamma2) via a comprehensive ligand-mapping approach. *J Med Chem* 2000;43(1):71–95. [PubMed: 10633039]
23. Li X, Cao H, Zhang C, Furtmueller R, Fuchs K, Huck S, Sieghart W, Deschamps J, Cook JM. Synthesis, in vitro affinity, and efficacy of a bis 8-ethynyl-4H-imidazo[1,5a]-[1,4]benzodiazepine analogue, the first bivalent alpha5 subtype selective BzR/GABA(A) antagonist. *J Med Chem* 2003;46(26):5567–70. [PubMed: 14667209]
24. Cook JB, Foster KL, Eiler WJ 2nd, McKay PF, Woods J 2nd, Harvey SC, Garcia M, Grey C, McCane S, Mason D, Cummings R, Li X, Cook JM, June HL. Selective GABAA alpha5 benzodiazepine inverse agonist antagonizes the neurobehavioral actions of alcohol. *Alcohol Clin Exp Res* 2005;29(8):1390–401. [PubMed: 16131846]
25. Albaugh PA, Marshall L, Gregory J, White G, Hutchison A, Ross PC, Gallagher DW, Tallman JF, Crago M, Cassella JV. Synthesis and biological evaluation of 7,8,9,10-tetrahydroimidazo[1,2-c]pyrido[3,4-e]pyrimidin-5(6H)-ones as functionally selective ligands of the benzodiazepine receptor site on the GABA(A) receptor. *J Med Chem* 2002;45(23):5043–51. [PubMed: 12408715]
26. Collins I, Moyes C, Davey WB, Rowley M, Bromidge FA, Quirk K, Atack JR, McKernan RM, Thompson SA, Wafford K, Dawson GR, Pike A, Sohal B, Tsou NN, Ball RG, Castro JL. 3-Heteroaryl-2-pyridones: benzodiazepine site ligands with functional delectivity for alpha 2/alpha 3-subtypes of human GABA(A) receptor-ion channels. *J Med Chem* 2002;45(9):1887–900. [PubMed: 11960500]
27. Mitchinson A, Atack JR, Blurton P, Carling RW, Castro JL, Curley KS, Russell MG, Marshall G, McKernan RM, Moore KW, Narquizian R, Smith A, Street LJ, Thompson SA, Wafford K. 2,5-Dihydropyrazolo[4,3-c]pyridin-3-ones: functionally selective benzodiazepine binding site ligands on the GABAA receptor. *Bioorg Med Chem Lett* 2004;14(13):3441–4. [PubMed: 15177449]



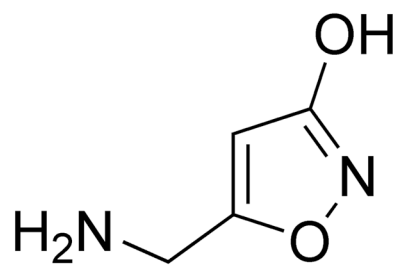
28. Yasumatsu H, Morimoto Y, Yamamoto Y, Takehara S, Fukuda T, Nakao T, Setoguchi M. The pharmacological properties of Y-23684, a benzodiazepine receptor partial agonist. *Br J Pharmacol* 1994;111(4):1170–8. [PubMed: 7913372]
29. Haefely W, Martin JR, Schoch P. Novel anxiolytics that act as partial agonists at benzodiazepine receptors. *Trends Pharmacol Sci* 1990;11(11):452–6. [PubMed: 1980040]
30. Grunwald C, Rundfeldt C, Lankau HJ, Arnold T, Hofgen N, Dost R, Egerland U, Hofmann HJ, Unverferth K. Synthesis, pharmacology, and structure-activity relationships of novel imidazolones and pyrrolones as modulators of GABAA receptors. *J Med Chem* 2006;49(6):1855–66. [PubMed: 16539371]
31. Krogsgaard-Larsen P, Frolund B, Jorgensen FS, Schousboe A. GABAA receptor agonists, partial agonists, and antagonists. Design and therapeutic prospects. *J Med Chem* 1994;37(16):2489–505. [PubMed: 8057295]
32. Rabe H, Picard R, Uusi-Oukari M, Hevers W, Lüddens H, Korpi ER. Coupling between agonist and chloride ionophore sites of the GABA(A) receptor: agonist/antagonist efficacy of 4-PIOL. *Eur J Pharmacol* 2000;409(3):233–42. [PubMed: 11108817]
33. Byberg JR, Labouta IM, Falch E, Hjeds H, Krogsgaard-Larsen P, Curtis DR, Gynther BD. Synthesis and biological activity of a GABAA agonist which has no effect on benzodiazepine binding and of structurally related glycine antagonists. *Drug Des Deliv* 1987;1(4):261–74. [PubMed: 2855566]
34. Frolund B, Jensen LS, Storustovu SI, Stensbol TB, Ebert B, Kehler J, Krogsgaard-Larsen P, Liljefors T. 4-aryl-5-(4-piperidyl)-3-isoxazolol GABAA antagonists: synthesis, pharmacology, and structure-activity relationships. *J Med Chem* 2007;50(8):1988–92. [PubMed: 17375905]
35. Krehan D, Storustovu SI, Liljefors T, Ebert B, Nielsen B, Krogsgaard-Larsen P, Frolund B. Potent 4-arylalkyl-substituted 3-isothiazolol GABA(A) competitive/noncompetitive antagonists: synthesis and pharmacology. *J Med Chem* 2006;49(4):1388–96. [PubMed: 16480274]
36. Frolund B, Jensen LS, Guandalini L, Canillo C, Vestergaard HT, Kristiansen U, Nielsen B, Stensbol TB, Madsen C, Krogsgaard-Larsen P, Liljefors T. Potent 4-aryl- or 4-arylalkyl-substituted 3-isoxazolol GABA(A) antagonists: synthesis, pharmacology, and molecular modeling. *J Med Chem* 2005;48(2):427–39. [PubMed: 15658856]
37. Frolund B, Tagmose L, Jorgensen AT, Kristiansen U, Stensbol TB, Liljefors T, Krogsgaard-Larsen P. Design and synthesis of a new series of 4-alkylated 3-isoxazolol GABA A antagonists. *Eur J Med Chem* 2003;38(4):447–9. [PubMed: 12750034]
38. Mortensen M, Frolund B, Jorgensen AT, Liljefors T, Krogsgaard-Larsen P, Ebert B. Activity of novel 4-PIOL analogues at human alpha 1 beta 2 gamma 2S GABA(A) receptors--correlation with hydrophobicity. *Eur J Pharmacol* 2002;451(2):125–32. [PubMed: 12231381]
39. Frolund B, Jorgensen AT, Tagmose L, Stensbol TB, Vestergaard HT, Engblom C, Kristiansen U, Sanchez C, Krogsgaard-Larsen P, Liljefors T. Novel class of potent 4-arylalkyl substituted 3-isoxazolol GABA(A) antagonists: synthesis, pharmacology, and molecular modeling. *J Med Chem* 2002;45(12):2454–68. [PubMed: 12036354]
40. Frolund B, Kristiansen U, Brehm L, Hansen AB, Krogsgaard-Larsen P, Falch E. Partial GABAA receptor agonists. Synthesis and in vitro pharmacology of a series of nonannulated analogs of 4,5,6,7-tetrahydroisoxazolo[5,4-c]pyridin-3-ol. *J Med Chem* 1995;38(17):3287–96. [PubMed: 7650683]
41. Akabas MH, Stauffer DA, Xu M, Karlin A. Acetylcholine receptor channel structure probed in cysteine-substitution mutants. *Science* 1992;258(5080):307–10. [PubMed: 1384130]
42. Sigel E, Baur R, Kellenberger S, Malherbe P. Point mutations affecting antagonist affinity and agonist dependent gating of GABA<sub>A</sub> receptor channels. *Embo J* 1992;11(6):2017–23. [PubMed: 1376242]
43. Hartvig L, Lukensmejer B, Liljefors T, Dekermendjian K. Two conserved arginines in the extracellular N-terminal domain of the GABA(A) receptor alpha(5) subunit are crucial for receptor function. *J Neurochem* 2000;75(4):1746–53. [PubMed: 10987858]
44. Westh-Hansen SE, Witt MR, Dekermendjian K, Liljefors T, Rasmussen PB, Nielsen M. Arginine residue 120 of the human GABAA receptor alpha 1, subunit is essential for GABA binding and chloride ion current gating. *Neuroreport* 1999;10(11):2417–21. [PubMed: 10439474]
45. Smith GB, Olsen RW. Identification of a [<sup>3</sup>H]muscimol photoaffinity substrate in the bovine gamma-aminobutyric acid A receptor alpha subunit. *J Biol Chem* 1994;269(32):20380–7. [PubMed: 8051133]

46. Holden JH, Czajkowski C. Different residues in the GABAA receptor alpha 1T60-alpha 1K70 region mediate GABA and SR-95531 actions. *J Biol Chem* 2002;277(21):18785–92. [PubMed: 11896052]
47. Boileau AJ, Evers AR, Davis AF, Czajkowski C. Mapping the agonist binding site of the GABA<sub>A</sub> receptor: evidence for a beta-strand. *J Neurosci* 1999;19(12):4847–54. [PubMed: 10366619]
48. Kloda JH, Czajkowski C. Agonist-, antagonist-, and benzodiazepine-induced structural changes in the alpha1 Met113-Leu132 region of the GABAA receptor. *Mol Pharmacol* 2007;71(2):483–93. [PubMed: 17108261]
49. Celie PH, van Rossum-Fikkert SE, van Dijk WJ, Brejc K, Smit AB, Sixma TK. Nicotine and carbamylcholine binding to nicotinic acetylcholine receptors as studied in AChBP crystal structures. *Neuron* 2004;41(6):907–14. [PubMed: 15046723]
50. Aranda G, Dessolin M, Golfier M, Guillerez MG. <sup>13</sup>C NMR Study of some Derivatives of 1,3,4-Oxadiazoles, 1,3,4-Thiadiazoles and Isosydnonones. *Org Magn Res* 1982;18:159–164.
51. Roberts DD, Lewis SD, Ballou DP, Olson ST, Shafer JA. Reactivity of small thiolate anions and Cysteine-25 in papain towards methylmethanethiosulfonate. *Biochemistry* 1986;25:5595–5601. [PubMed: 3778876]
52. Horenstein J, Akabas MH. Location of a high affinity Zn<sup>2+</sup> binding site in the channel of alpha1beta1 gamma-aminobutyric acid A receptors. *Mol Pharmacol* 1998;53(5):870–7. [PubMed: 9584213]
53. Baumann SW, Baur R, Sigel E. Subunit arrangement of gamma-aminobutyric acid type A receptors. *J Biol Chem* 2001;276(39):36275–80. [PubMed: 11466317]
54. Frolund B, Tagmose L, Liljefors T, Stensbol TB, Engblom C, Kristiansen U, Krosggaard-Larsen P. A novel class of potent 3-isoxazolol GABA(A) antagonists: design, synthesis, and pharmacology. *J Med Chem* 2000;43(26):4930–3. [PubMed: 11150163]
55. Krosggaard-Larsen P, Mikkelsen H, Jacobsen P, Falch E, Curtis DR, Peet MJ, Leah JD. 4,5,6,7-Tetrahydroisothiazolo[5,4-c]pyridin-3-ol and related analogues of THIP. Synthesis and biological activity. *J Med Chem* 1983;26(6):895–900. [PubMed: 6304315]
56. Brejc K, van Dijk WJ, Smit AB, Sixma TK. The 2.7 Å structure of AChBP, homologue of the ligand-binding domain of the nicotinic acetylcholine receptor. *Novartis Found Symp* 2002;245:22–9. [PubMed: 12027010]discussion 29–32, 165–8
57. Cromer BA, Morton CJ, Parker MW. Anxiety over GABA(A) receptor structure relieved by AChBP. *Trends Biochem Sci* 2002;27(6):280–7. [PubMed: 12069787]
58. Brejc K, van Dijk WJ, Klaassen RV, Schuurmans M, van Der Oost J, Smit AB, Sixma TK. Crystal structure of an ACh-binding protein reveals the ligand-binding domain of nicotinic receptors. *Nature* 2001;411(6835):269–76. [PubMed: 11357122]
59. Wagner DA, Czajkowski C. Structure and dynamics of the GABA binding pocket: A narrowing cleft that constricts during activation. *J Neurosci* 2001;21(1):67–74. [PubMed: 11150321]
60. Jin R, Banke TG, Mayer ML, Traynelis SF, Gouaux E. Structural basis for partial agonist action at ionotropic glutamate receptors. *Nat Neurosci* 2003;6(8):803–10. [PubMed: 12872125]
61. Aboul-Enein MN, Azzouny AA, Abdallah NA, El-Shabrawy Makhlof AA, Werner W. Synthesis of Certain 5-Piperidyl-1,3,4-Oxadiazol-2(3H)-ones and -2(3H)-thiones having Nonulcerogenic. Antiinflammatory and Analgesic Activities. *Sci Pharm* 1995;(63):175–190.
62. Bentley KW, Burton M, Uff BC. 1,3,4-Oxadiazol-2(3H)-one Formation from N-Acylaminobiurets and Related Compounds and from S-Benzyl 3-Acyl(thiocarbazates). *J Chem Soc Perkin Trans I* 1982;9:2019–2021.
63. Dornow AKB. Notiz über die Darstellung von 1.3.4-Oxadiazolon-(5) und seinen C2-alkylierten Derivaten. *Chem Ber* 1949;82:121–123.
64. Hoggarth E. 2-Benzoyldithiocarbazine Acid and Related Compounds. *J Chem Soc Perkin Trans I* 1952:4811–4817.
65. Horning DE, Muchowski JM. Five-membered Heterocyclic Thiones. Part I. 1,3,4-Oxadiazol-2-thione. *Can J Chem* 1972;50:3079–3083.
66. Korpi ER, Luddens H. Regional gamma-aminobutyric acid sensitivity of t-butylbicyclophosphoro [35S]thionate binding depends on gamma-aminobutyric acidA receptor alpha subunit. *Mol Pharmacol* 1993;44(1):87–92. [PubMed: 8393526]
67. Luddens H, Korpi ER. GABA antagonists differentiate between recombinant GABAA/benzodiazepine receptor subtypes. *J Neurosci* 1995;15(10):6957–62. [PubMed: 7472452]

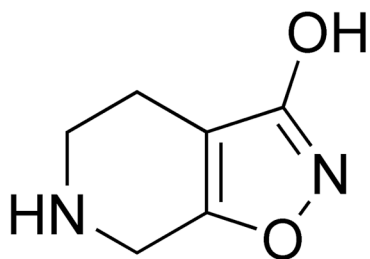
68. Pritchett DB, Seeburg PH. Gamma-aminobutyric acidA receptor alpha 5-subunit creates novel type II benzodiazepine receptor pharmacology. *J Neurochem* 1990;54(5):1802–4. [PubMed: 2157817]
69. Hamill OP, Marty A, Neher E, Sakmann B, Sigworth FJ. Improved patch-clamp techniques for high-resolution current recording from cells and cell-free membrane patches. *Pflugers Arch* 1981;391(2):85–100. [PubMed: 6270629]
70. Horenstein J, Wagner DA, Czajkowski C, Akabas MH. Protein mobility and GABA-induced conformational changes in GABA<sub>A</sub> receptor pore-lining M2 segment. *Nat Neurosci* 2001;4(5):477–85. [PubMed: 11319555]
71. Schwede T, Kopp J, Guex N, Peitsch MC. SWISS-MODEL: An automated protein homology-modeling server. *Nucleic Acids Res* 2003;31(13):3381–5. [PubMed: 12824332]
72. Bali M, Akabas MH. Defining the propofol binding site location on the GABAA receptor. *Mol Pharmacol* 2004;65(1):68–76. [PubMed: 14722238]



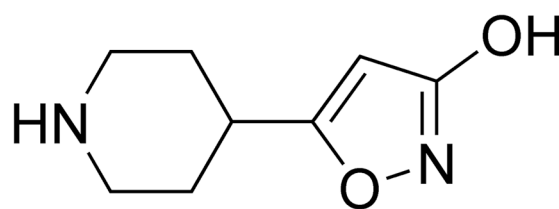
GABA



muscimol

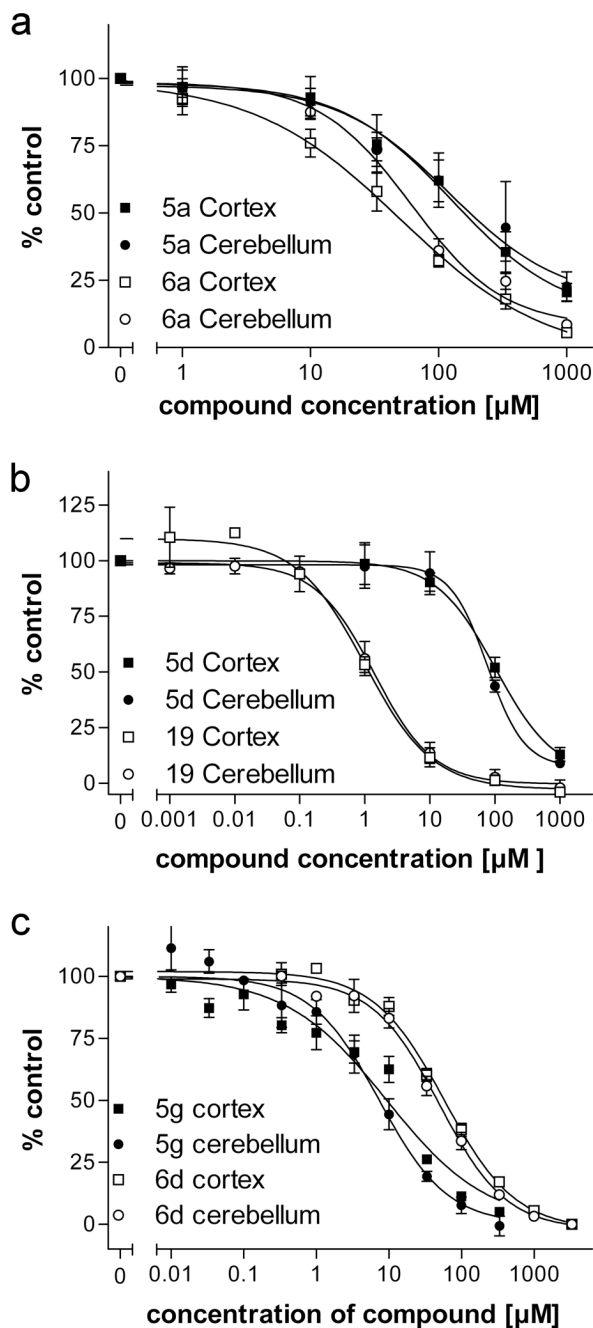


THIP



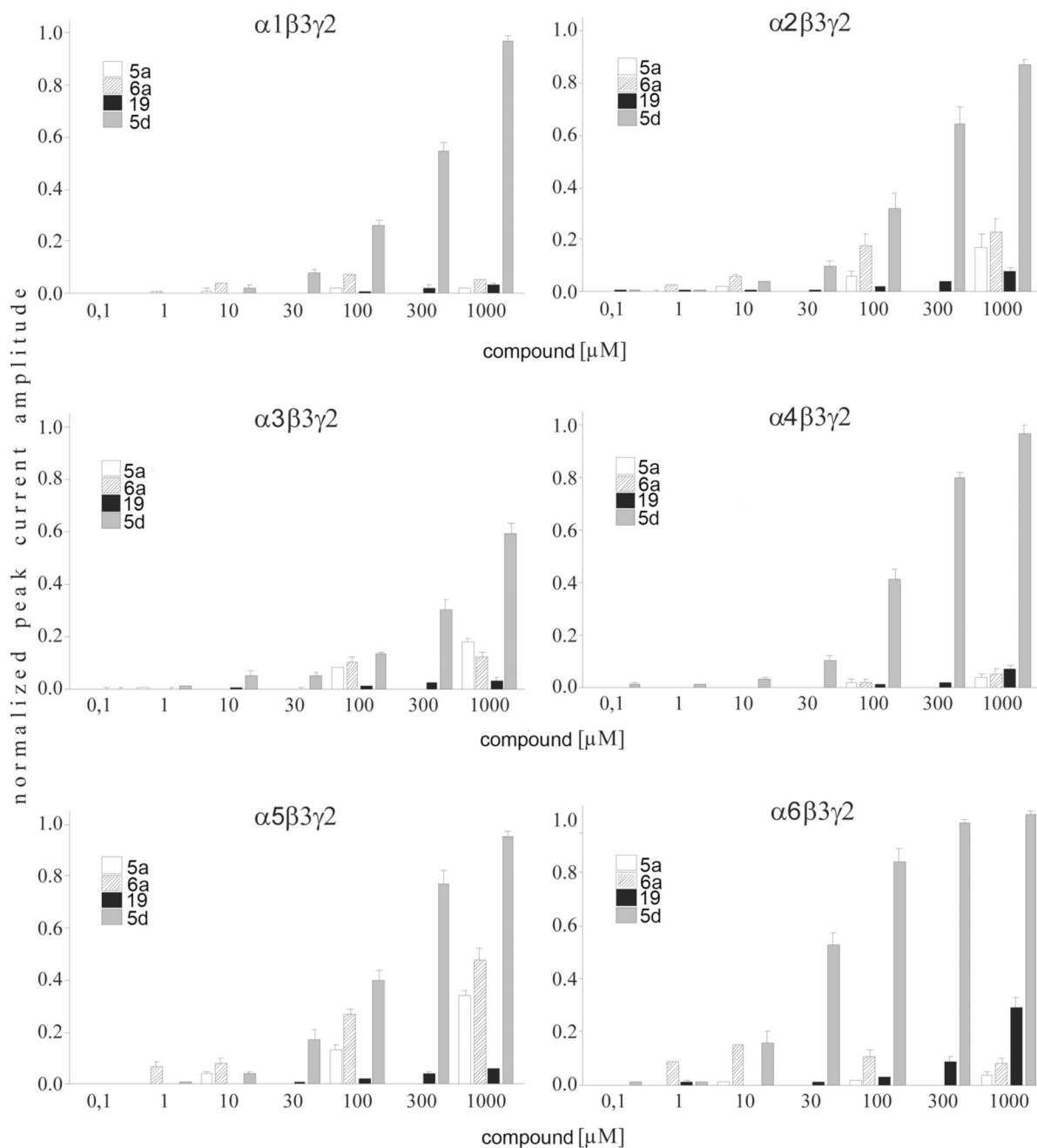
4-PIOL

**Figure 1.**  
Structures of GABA, muscimol, THIP and 4-PIOL.

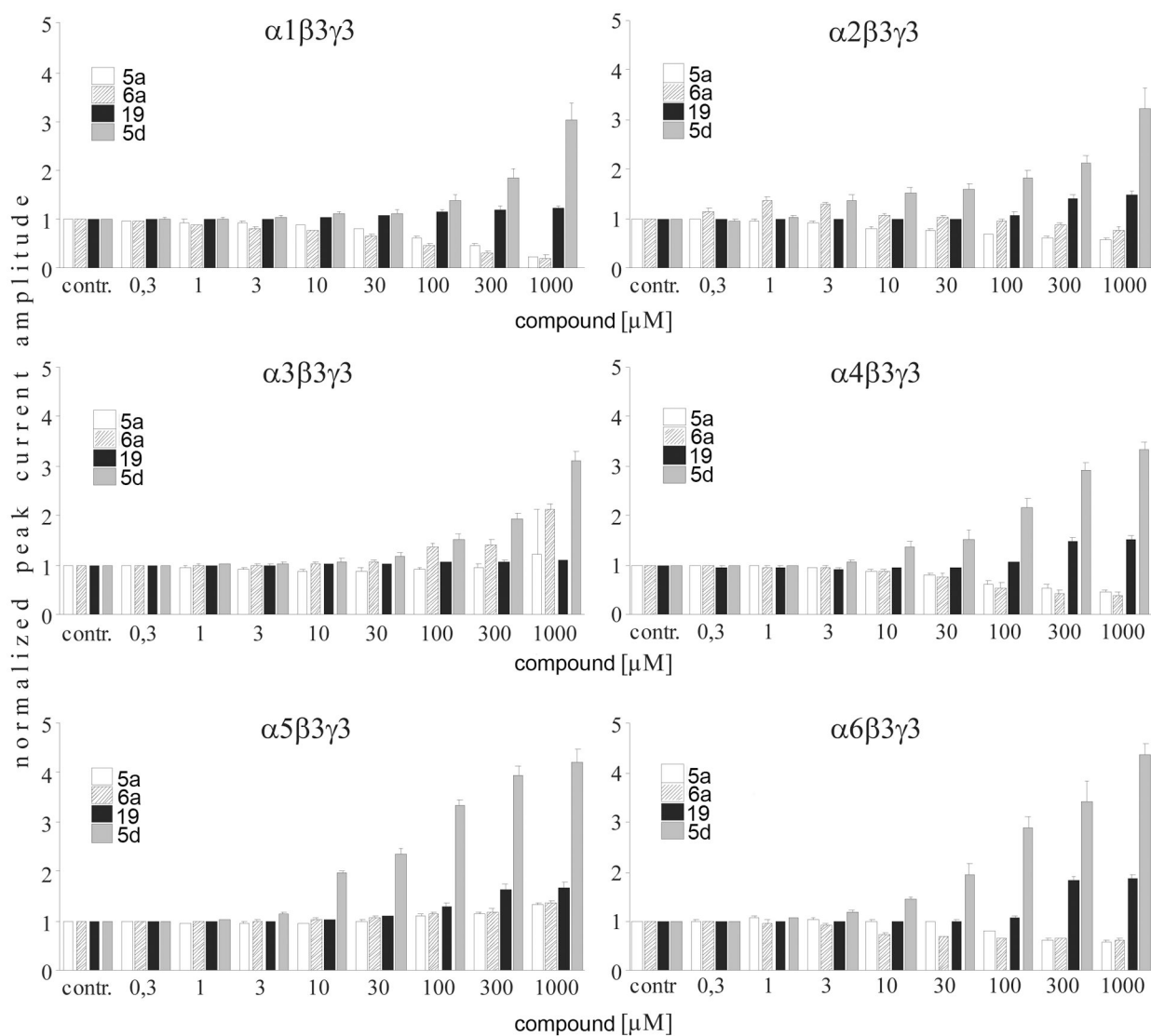


**Figure 2.** Dose-response curves as measured against [ $^3\text{H}$ ]muscimol binding to cortical (squares) and cerebellar (circles) membranes. Binding data were normalized to the binding in the absence of any inhibitor set to 100%. Error bars indicate the S.E.M for at least three independent tissue preparations.

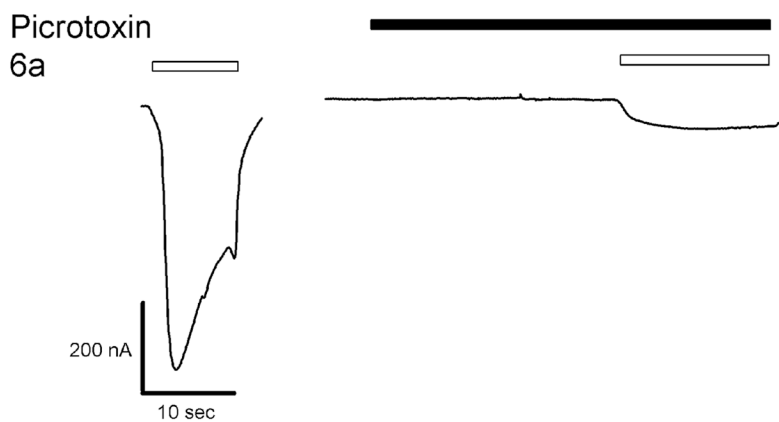


**Figure 3.**

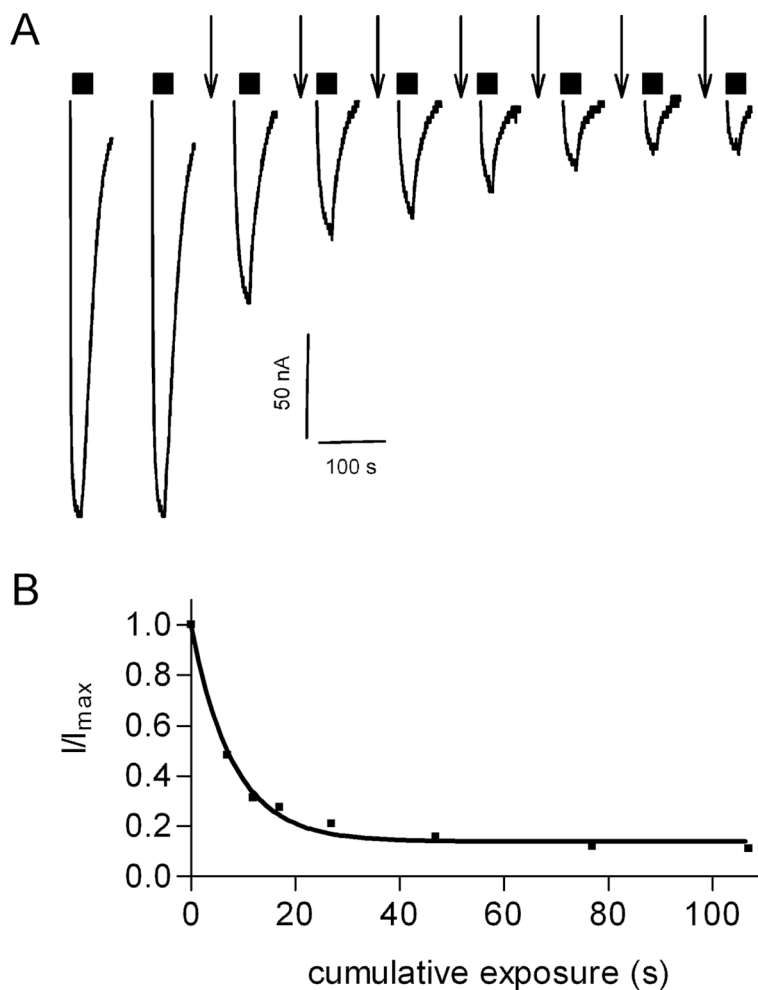
Whole-cell recordings of HEK 293 cells expressing recombinant rat  $\alpha_i\beta_3\gamma_2$  ( $i = 1-6$ ) GABA<sub>A</sub> receptors. Currents were normalized to the maximally GABA-induced current at the approximate EC<sub>100</sub>. To test the intrinsic activity, different concentrations of the 5-(4-piperidyl)-1,3,4-oxadiazol-derivates tested were applied to the cells. Error bars indicate the S.E.M for at least four cells.



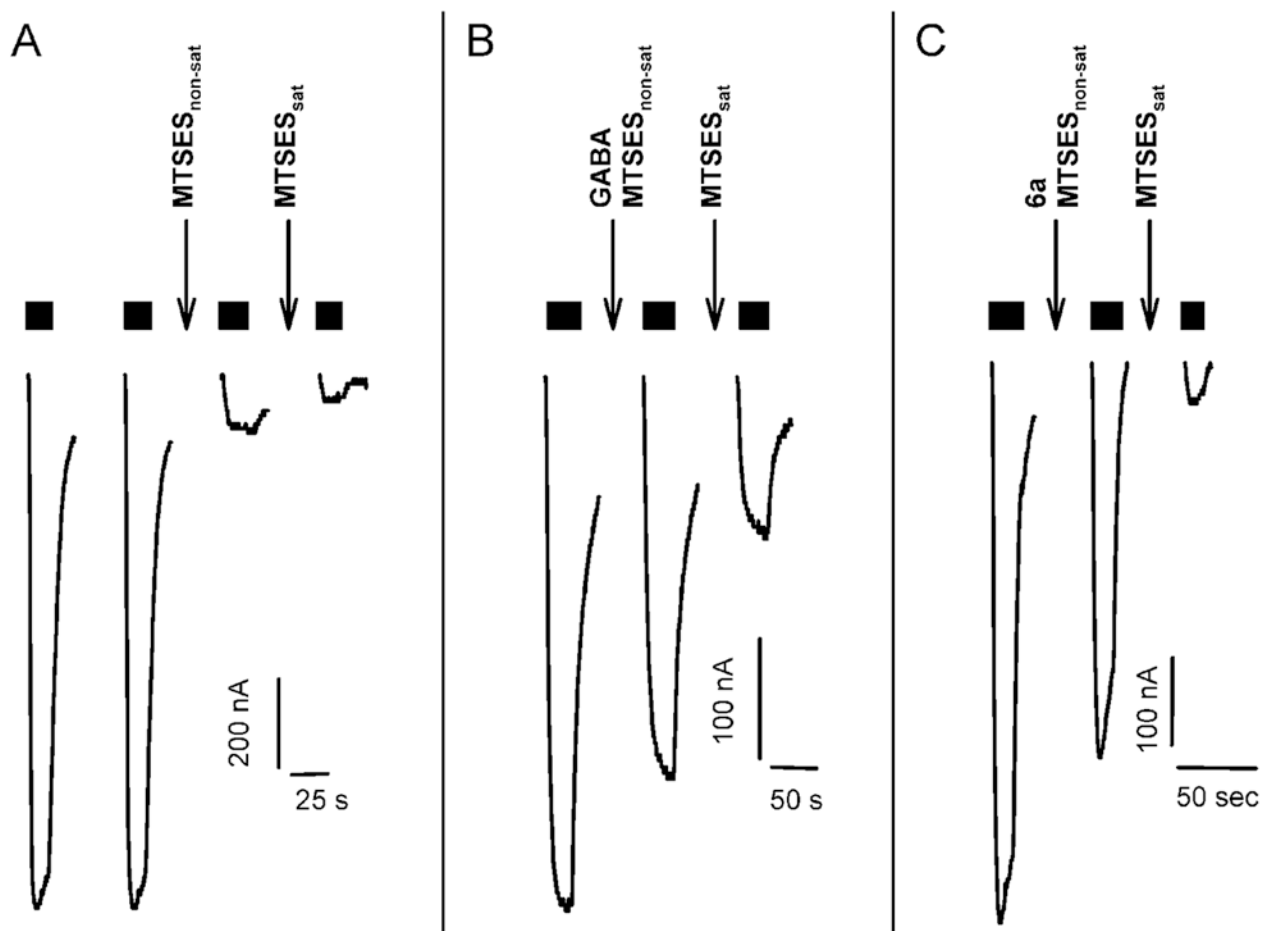
**Figure 4.** Whole-cell recordings of HEK 293 cells expressing recombinant rat  $\alpha_i\beta_3\gamma_2$  ( $i = 1-6$ ) GABA<sub>A</sub> receptors. Currents were normalized to the GABA concentrations specific for the receptor subtype under *in vitro* conditions. Different concentrations of the 5-(4-piperidyl)-1,3,4-oxadiazol-derivates tested were co-applied with GABA concentrations around the EC<sub>25</sub>. Error bars indicate the S.E.M. for at least four cells.



**Figure 5.** Picrotoxin blocks **6a** induced currents in  $\alpha_1\beta_2$  wt receptors. The first trace shows a **6a** induced current. The second trace was recorded during a 20 s application of picrotoxin, immediately followed by a co-application of **6a** and picrotoxin.



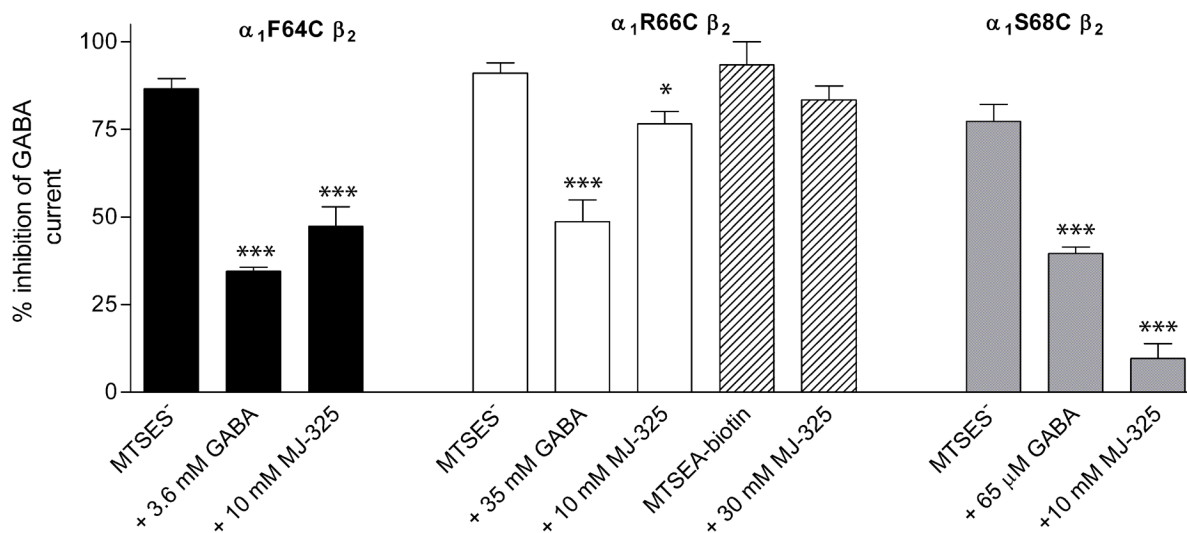
**Figure 6.** MTSES<sup>-</sup> reaction rate with the  $\alpha_1$ F64C $\beta_2$  cysteine mutant. **A**, EC<sub>50</sub> GABA current traces were recorded initially and after each brief application of 10  $\mu$ M MTSES<sup>-</sup> ( $\downarrow$ ). Currents during MTSES<sup>-</sup> application ( $\downarrow$ ) are not shown. **B**, GABA test currents were normalized to the initial GABA current (I<sub>max</sub>) and plotted versus cumulative MTSES<sup>-</sup> exposure time. Data were fit to a monoexponential decay function.



**Figure 7.**

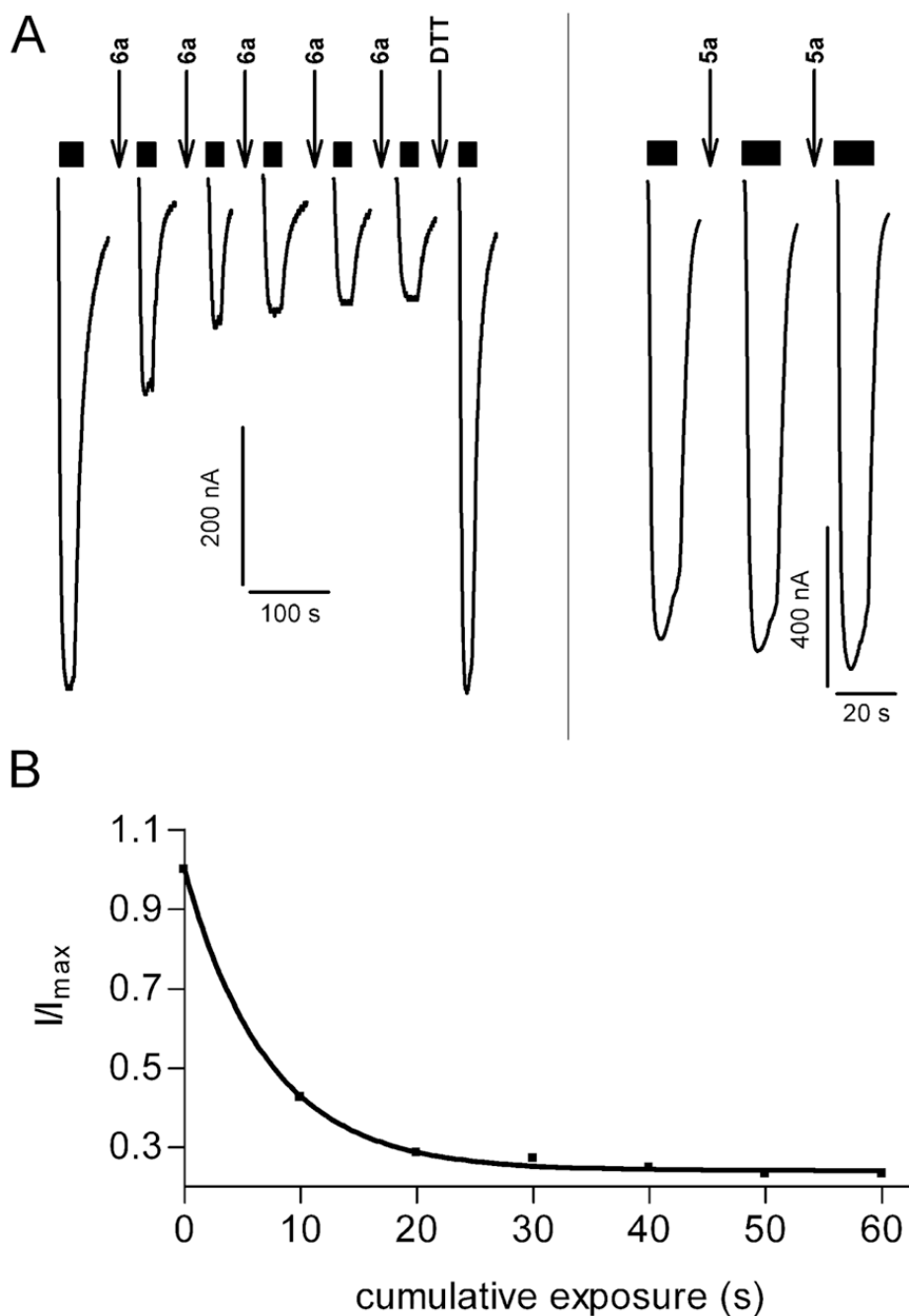
Protection assay shows that GABA and **6a** protect  $\alpha_1\text{F64C}\beta_2$  receptors from reaction with  $\text{MTSESE}^-$ . **A**,  $\text{MTSESE}^-$  modification of  $\alpha_1\text{F64C}\beta_2$  in the absence of agonist. Two GABA test pulses were applied to demonstrate the stability of the GABA current. At the downward arrow marked  $\text{MTSESE}_{\text{non-sat}}$   $10 \mu\text{M}$   $\text{MTSESE}^-$  was applied for 12 s. Following washout a GABA test pulse was recorded. The GABA test current (third trace) was reduced by 87%. At the downward arrow marked  $\text{MTSESE}_{\text{sat}}$   $20 \mu\text{M}$   $\text{MTSESE}^-$  was applied for 50 s to bring the  $\text{MTSESE}^-$  reaction to completion. Following washout a final GABA test pulse (fourth trace) was applied. Currents during  $\text{MTSESE}^-$  applications ( $\downarrow$ ) are not shown. **B**, GABA protects  $\alpha_1\text{F64C}\beta_2$  from modification by  $\text{MTSESE}^-$ . The same series of reagents are applied as in panel A, except that the  $\text{MTSESE}_{\text{non-sat}}$  was coapplied with  $3.6 \text{ mM}$  GABA. The GABA current elicited by the next GABA test pulse (middle trace) is significantly larger than the GABA current after the  $\text{MTSESE}_{\text{non-sat}}$  application in panel A, indicating that the presence of GABA significantly reduced the extent of reaction with the non-saturating concentration of  $\text{MTSESE}^-$ . **C**, **6a** protects  $\alpha_1\text{F64C}\beta_2$  from modification by  $\text{MTSESE}^-$ . The same series of reagents are applied as in panel A, except that the  $\text{MTSESE}_{\text{non-sat}}$  was coapplied with  $10 \text{ mM}$  **6a**. The GABA current elicited by the next GABA test pulse (middle trace) is significantly larger than the GABA current after the  $\text{MTSESE}_{\text{non-sat}}$  application in panel A, indicating that the presence of **6a** significantly reduced the extent of reaction with the non-saturating concentration of  $\text{MTSESE}^-$ . Currents during  $\text{MTSESE}^-$  application ( $\downarrow$ ) with or without agonist are not shown. Duration of application of GABA  $\text{EC}_{50}$  test pulses are indicated by black horizontal bars above the current traces.





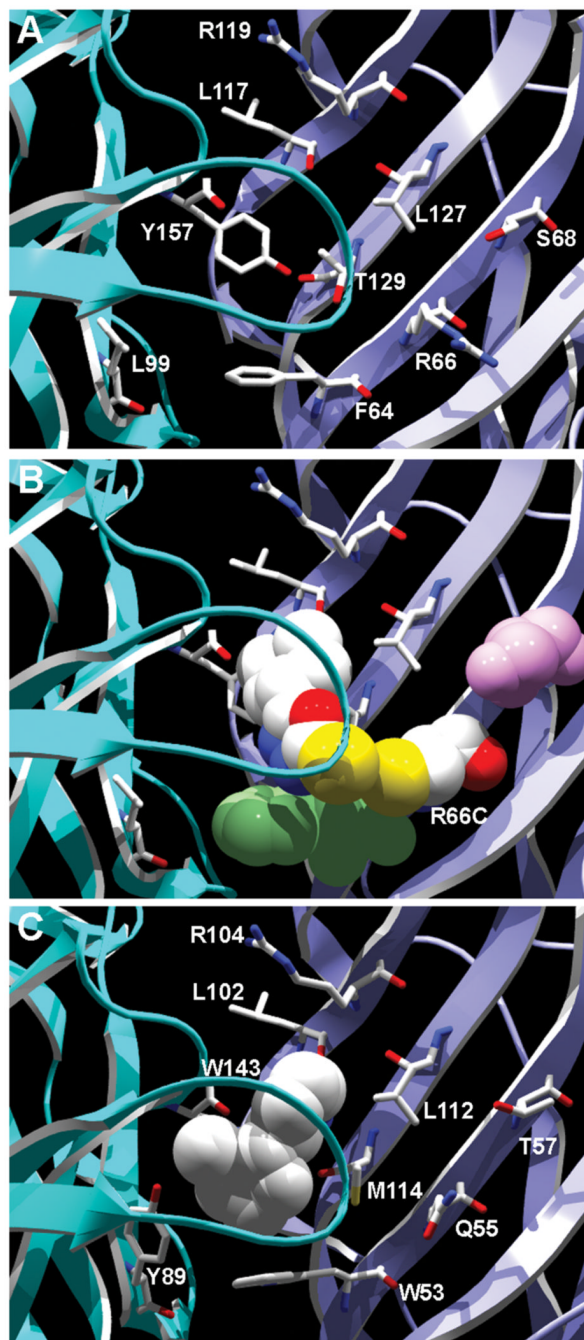
**Figure 8.**

Summary of the protection assay with  $\alpha_1$ F64C $\beta_2$  (black bars),  $\alpha_1$ R66C $\beta_2$  (clear and striped bars), and  $\alpha_1$ S68C $\beta_2$  (grey bars). Bars indicate the average percent inhibition of GABA test currents following the application of a non-saturating concentration of MTSES<sup>-</sup> either in the absence of agonist or in the presence of EC<sub>90</sub> GABA or **6a** (10 or 30 mM). We infer that a reagent, GABA or **6a**, protected a mutant from reaction with MTSES<sup>-</sup> if the extent of inhibition by MTSES<sup>-</sup> coapplied with either GABA or **6a** is significantly less than the extent of inhibition by MTSES<sup>-</sup> applied alone. Conditions where the co-application of GABA or **6a** are significantly different than the effect of MTSES<sup>-</sup> application alone are indicated by \*; (\*, P<0.014; \*\*\*, P<0.0001) by one way ANOVA and Fisher's PLSD. For  $\alpha_1$ R66C $\beta_2$  30  $\mu$ M MTSEA-biotin reduced the subsequent GABA test currents by 93%. Application of 30  $\mu$ M MTSEA-biotin with 30 mM **6a** reduced the subsequent GABA test currents by 83%. The limited supply of **6a** precluded further experiments.



**Figure 9.** **6a** reacted with  $\alpha_1R66C\beta_2$ . **A**, Currents recorded from an oocyte expressing  $\alpha_1R66C\beta_2$ . Alternating 10-s applications of 30 mM **6a** [indicated by ( $\downarrow$ )] and 5.5 mM GABA test currents (bars above current traces) resulted in a progressive decrease in the GABA test currents. The decrease eventually plateaued at which time a 12-s application of 10 mM MTSES<sup>-</sup> ( $\downarrow$ ) had no effect indicating that all accessible cysteine had reacted with **6a**. Reduction by a 20-s application of 10 mM DTT ( $\downarrow$ ) led to complete recovery of the GABA test current magnitude. Currents during application of **6a**, MTSES<sup>-</sup> and DTT are not shown. **B**, Application of the oxygen analogue **5a** (30 mM, 10 s) ( $\downarrow$ ) to an oocyte expressing  $\alpha_1R66C\beta_2$  did not decrease the subsequent GABA test currents. Currents during **5a** application are not shown. **C**, Reaction

rate of **6a** with  $\alpha_1R66C\beta_2$ . GABA test currents were normalized to the initial GABA test current, plotted as a function of cumulative duration of **6a** application and fitted to a monoexponential decay function.

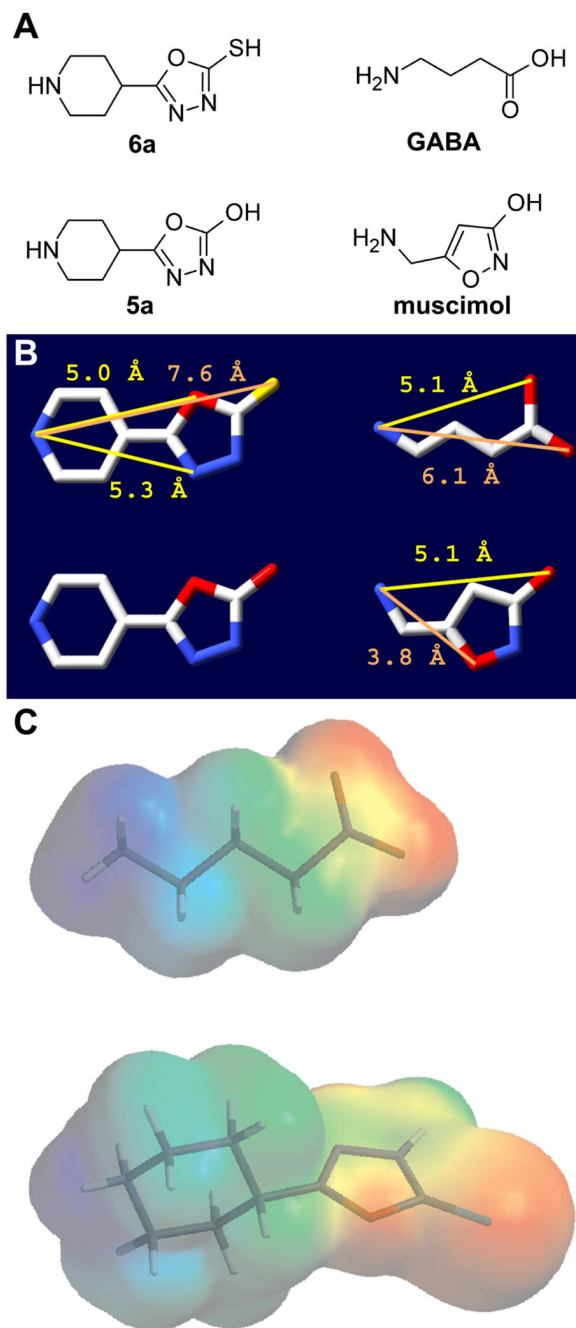


**Figure 10.**

Homology model of the GABA<sub>A</sub> receptor agonist binding site based on the AChBP structure (PDB 1UW6). **A**, View of the principle side of the  $\beta_2$  subunit GABA binding site (light blue) and of the complementary side of the  $\alpha_1$  subunit GABA binding site (dark blue) showing backbone in ribbon form. Side chains of residues mentioned in the text are shown in wireframe format. **B**, GABA binding site showing backbone in ribbon form with **6a** and  $\alpha_1$ R66C shown in spacefilling format with CPK colors. The close proximity of the sulfurs (yellow) in **6a** and  $\alpha_1$ Cys66 is consistent with the observed reaction between **6a** and  $\alpha_1$ Cys66.  $\alpha_1$ F64 is shown in green spacefilling format. The close proximity between  $\alpha_1$ F64 and **6a** is consistent with the steric protection of the cysteine substituted at this position. In contrast,  $\alpha_1$ S68 (pink colored

spacefilling format) is not in close proximity to **6a**. **C**, View of nicotine bound in the AChBP binding site (PDB 1UW6) from the same perspective as in panel B. Backbone is shown in ribbon form and nicotine in white-color spacefilling format. Side chains of AChBP residues aligned with the GABA<sub>A</sub> cysteine mutants discussed in the text and shown in panel C are in wireframe format. Nicotine interacts with the homologous  $\beta$  strand adjacent to the  $\beta$  strand containing the residue in this model aligned with GABA<sub>A</sub>  $\alpha_1$ R66.

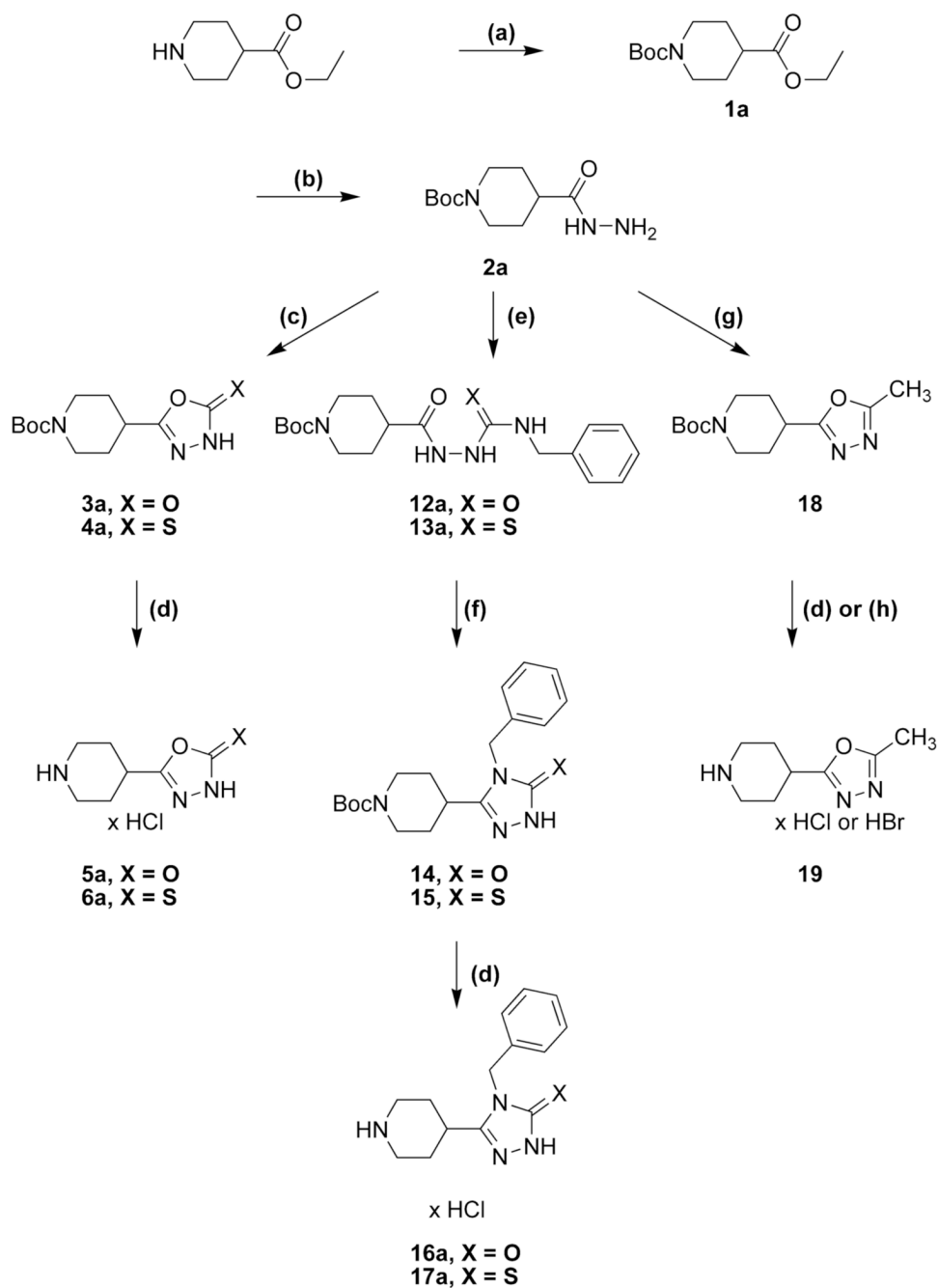




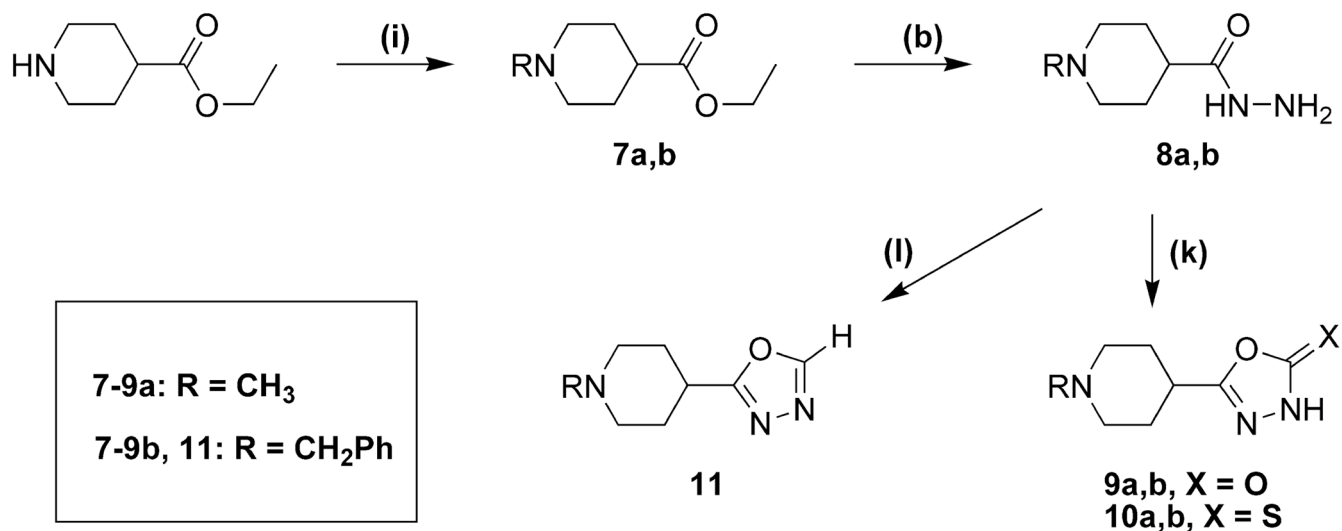
**Figure 11.**

**A**, Structures of **6a** and **5a** (left column) and of GABA and muscimol (right column). **B**, Structures of the compounds in panel A with atomic distances between the basic nitrogen atom and other polar atoms in the respective molecules. Distances were measured after energy minimization (Chemsketch 5.12, ACD Inc., Toronto, Ontario, Canada). CPK color scheme used, carbon, white; nitrogen, blue; oxygen, red; sulfur, yellow. **C**, Electrostatic potential mapped onto the van der Waals surface of GABA (top) and **6a** (bottom) with stick representation of molecules. Red indicates negative electrostatic potential and blue is positive potential. Image generated using Spartan. Note the similarity of the overall electrostatic

potential, especially the distance between the positively charged nitrogen in GABA or **6a** to the negative carboxylate (GABA) or the oxadiazolthione moiety (**6a**).

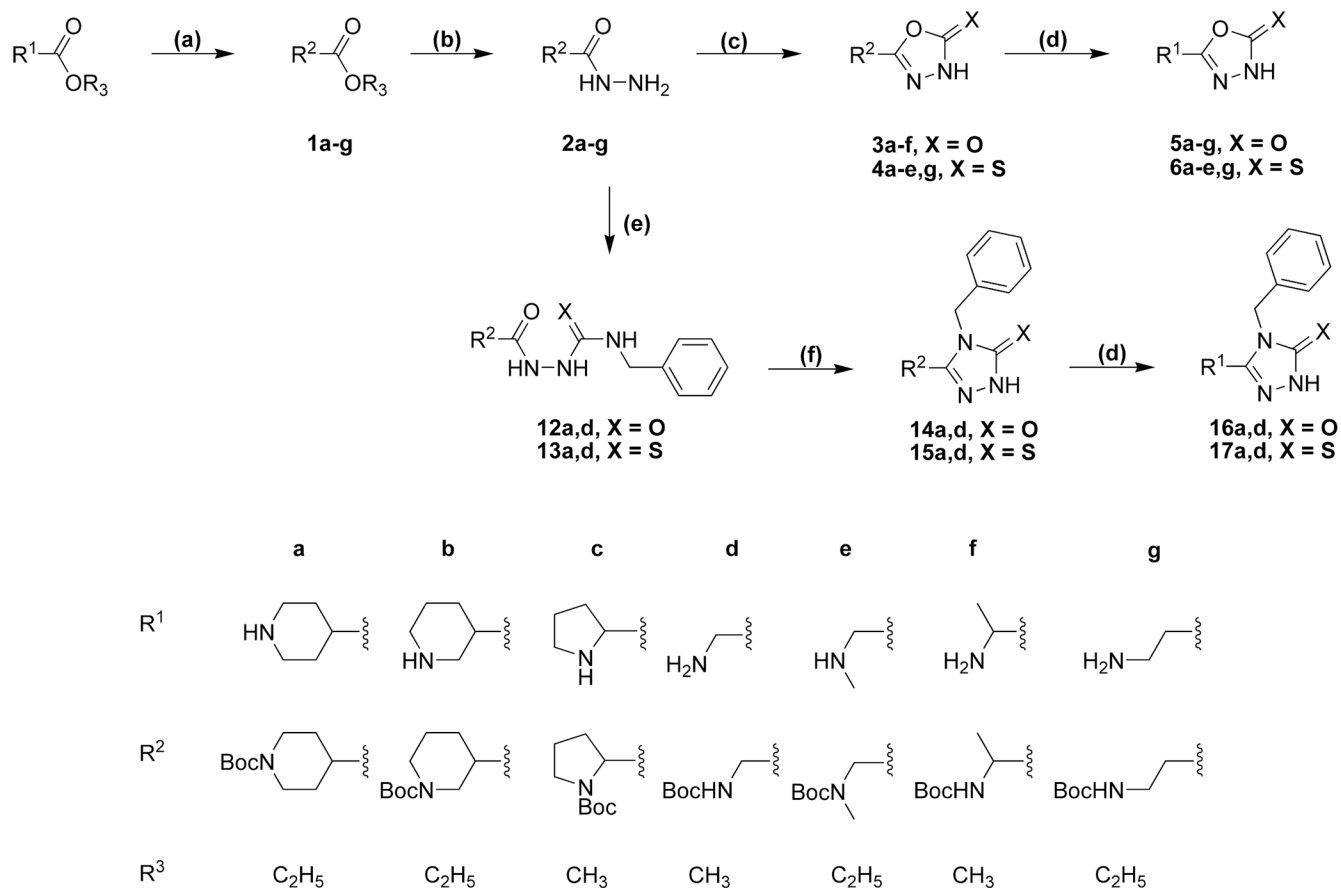
**Scheme 1a.**

<sup>a</sup> Reaction conditions: (a) Et<sub>3</sub>N, Boc<sub>2</sub>O in CH<sub>2</sub>Cl<sub>2</sub> or NaHCO<sub>3</sub>, Boc<sub>2</sub>O in water; (b) NH<sub>2</sub>NH<sub>2</sub>; (c) CDI to obtain **3**; CS<sub>2</sub> to obtain **4**; (d) 2.3 N ethanolic HCl; (e) PhCH<sub>2</sub>NCX; (f) 2% NaOH; (g) H<sub>3</sub>CC(OC<sub>2</sub>H<sub>5</sub>)<sub>3</sub>; (h) HBr/HAc.

**Scheme 2a.**

<sup>a</sup> Reaction conditions: (b) NH<sub>2</sub>NH<sub>2</sub>; (i) CH<sub>2</sub>O, HCOOH to obtain **7a**; PhCH<sub>2</sub>Cl to obtain **7b**;

(k) triphosgene to obtain **9a,b**; CS<sub>2</sub> to obtain **10a,b**; (l) HC(OC<sub>2</sub>H<sub>5</sub>)<sub>3</sub>.

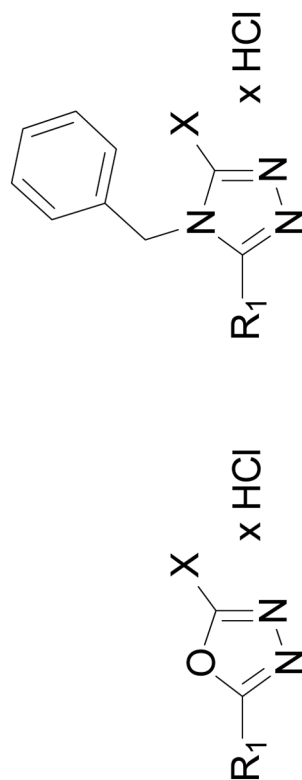
**Scheme 3a.**

<sup>a</sup> Reaction conditions as given in Scheme 1 and Scheme 2.





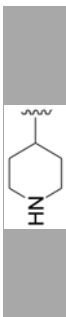



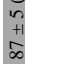
Percent inhibition of [<sup>3</sup>H]muscimol binding to well-washed membranes from rat cortex and cerebellum by 100 μM and 1 mM of test compounds. Given are the means ± S.D. with the number of experiments in brackets. Compound **17a** was insoluble at 1 mM and therefore not tested at this concentration. Structure I applies except where II is specifically indicated. Compounds for which an IC<sub>50</sub> is reported in Table 2 are shaded grey.



#	R	I		II		cerebellum	
		X	100 μM	cortex	1 Mm	100 μM	1 mM
<b>5a</b>		OH	38 ± 15 (4)		79 ± 7 (4)	38 ± 20 (4)	77 ± 11 (4)
<b>5b</b>		OH	1 ± 11 (3)		24 ± 5 (4)	9 ± 9 (4)	10 ± 7 (4)
<b>5c</b>		OH	5 ± 7 (3)		10 ± 3 (3)	8 ± 1 (3)	13 ± 4 (3)
<b>5d</b>		OH	99 ± 4 (3)		104 ± 2 (3)	97 ± 6 (3)	102 ± 6 (3)
<b>5e</b>		OH	14 ± 3 (3)		58 ± 4 (3)	22 ± 3 (3)	64 ± 1 (3)
<b>5f</b>		OH	26 ± 25 (3)		16 ± 4 (3)	13 ± 17 (3)	34 ± 4 (3)
<b>5g</b>		OH	85 ± 5 (3)		100 ± 1 (3)	89 ± 1 (3)	98 ± 0 (3)
<b>6a</b>		SH	68 ± 5 (4)		94 ± 2 (4)	64 ± 9 (4)	91 ± 2 (4)



#	R	I		II		cortex		cerebellum	
		X	x HCl	100 $\mu$ M	1 Mm	100 $\mu$ M	1 mM	100 $\mu$ M	1 mM
10a		SH	x HCl	6 $\pm$ 6 (4)	48 $\pm$ 6 (4)	8 $\pm$ 10 (4)	27 $\pm$ 8 (4)		
10b		SH	x HCl	3 $\pm$ 13 (4)	33 $\pm$ 14 (4)	6 $\pm$ 2 (4)	30 $\pm$ 5 (4)		
10c		SH	x HCl	22 $\pm$ 8 (3)	47 $\pm$ 7 (3)	3 $\pm$ 8 (3)	37 $\pm$ 6 (3)		
10d		SH	x HCl	10 $\pm$ 1 (3)	18 $\pm$ 2 (3)	0 $\pm$ 8 (3)	-3 $\pm$ 3 (3)		
10e		SH	x HCl	20 $\pm$ 4 (3)	10 $\pm$ 1 (3)	-4 $\pm$ 4 (3)	-3 $\pm$ 10 (3)		
11		H		-5 $\pm$ 3 (3)	1 $\pm$ 1 (3)	1 $\pm$ 3 (3)	-5 $\pm$ 4 (3)		
16a (II)		OH		18 $\pm$ 3 (3)	56 $\pm$ 3 (3)	14 $\pm$ 1 (3)	52 $\pm$ 2 (3)		
16d (II)		OH		4 $\pm$ 3 (3)	11 $\pm$ 1 (3)	1 $\pm$ 4 (3)	2 $\pm$ 4 (3)		
17a (II)		SH		-6 $\pm$ 11 (3)	-	13 $\pm$ 18 (3)	-		
17d (II)		SH		*	*	*	*		*

#	R	I		II		cerebellum	1 mM	100 μM	1 mM		
		X	R <sub>1</sub>	X	R <sub>1</sub>						
19								48 ± 8 (3)	87 ± 5 (3)	56 ± 5 (3)	91 ± 1 (3)

\* inactive.



Binding parameters of selected compounds against 6 nM [<sup>3</sup>H]muscimol in crude membrane preparations of rat cortex and cerebellum determined by nonlinear regression. Given are the means ± S.E.M. of the decadic logarithm of the IC<sub>50</sub> in μM, the corresponding pseudo-Hill coefficient η and the number of experiments n.

Table 2

	Cortex			Cerebellum				
	lg IC <sub>50</sub>	IC <sub>50</sub> [μM]	η	n	lg IC <sub>50</sub>	IC <sub>50</sub> [μM]	η	n
<b>5a</b>	2.262 ± 0.185	183	0.86 ± 0.10	4	2.089 ± 0.170	123	0.79 ± 0.06	3
<b>5d</b>	0.139 ± 0.119	1.4	1.12 ± 0.13	3	0.048 ± 0.082	1.1	0.90 ± 0.21	3
<b>5g</b>	0.971 ± 0.074	9.4	0.63 ± 0.06	4	0.868 ± 0.065	7.4	0.92 ± 0.11	3
<b>6a</b>	1.668 ± 0.153	47	0.99 ± 0.09	3	1.819 ± 0.048	66	1.03 ± 0.08	4
<b>6d</b>	1.758 ± 0.074	57	0.92 ± 0.05	3	1.690 ± 0.081	49	0.96 ± 0.12	4
<b>19</b>	2.039 ± 0.067	109	0.88 ± 0.08	3	1.879 ± 0.081	76	0.91 ± 0.05	3

**Table 3**

GABA concentrations and the corresponding relative effective concentration that induces a response around the EC<sub>20</sub> when applied to GABA<sub>A</sub> receptors  $\alpha_i\beta_3\gamma_2$  (i=1–6) transiently expressed in HEK 293 cells. Given are the mean  $\pm$  S.E.M.

<b><math>\alpha</math>subunit</b>	<b>GABA [<math>\mu</math>M]</b>	<b>EC</b>
$\alpha_1$	2.0	25 $\pm$ 2.3
$\alpha_2$	4.0	24 $\pm$ 1.9
$\alpha_3$	8.0	22 $\pm$ 2.1
$\alpha_4$	5.0	25 $\pm$ 2.0
$\alpha_5$	3.0	22 $\pm$ 2.1
$\alpha_6$	0.5	20 $\pm$ 2.2

**Table 4**

Maximal intrinsic activity of 1 mM **5d** normalized to the approximate maximal GABA-induced current ( $I/I_{\max\text{GABA}}$ ) and the **5d**  $EC_{50}$  and Hill coefficient on  $\alpha_i\beta_3\gamma_2$  ( $i=1-6$ )  $GABA_A$  receptors. Data are means  $\pm$  S.E.M.

$\alpha$ subunit	$I/I_{\max\text{GABA}}$	$EC_{50}$ [ $\mu\text{M}$ ]	Hill
$\alpha_1$	$0.93 \pm 0.03$	$280 \pm 17$	$0.99 \pm 0.05$
$\alpha_2$	$0.88 \pm 0.02$	182 *	1.23 *
$\alpha_3$	$0.59 \pm 0.04$	2300 *	0.81 *
$\alpha_4$	$0.97 \pm 0.01$	$128 \pm 8$	$1.56 \pm 0.11$
$\alpha_5$	$0.95 \pm 0.03$	$137 \pm 14$	$1.31 \pm 0.12$
$\alpha_6$	$1.03 \pm 0.01$	$30 \pm 3$	$1.41 \pm 0.14$

\* marks values of an extrapolated dose-response curve.

**Table 5**  
Summary of dose-response data and **6a** competition data using a GABA EC<sub>20</sub> concentration from cysteine-substituted and wt  $\alpha_1\beta_2$  GABAA receptors.

Receptor	GABA			6a			
	EC <sub>50</sub> ( $\mu$ M)	mutant/wt	n	EC <sub>50</sub> (mM)	n	IC <sub>50</sub> ( $\mu$ M)	n
$\alpha_1\beta_2$ wt	10.0 $\pm$ 1.2	1	6	9.5 $\pm$ 0.02	2	59 $\pm$ 6	4
$\alpha_1$ F64C $\beta_2$	430 $\pm$ 40	43	6	5.5 $\pm$ 0.2	4	56 $\pm$ 12	3
$\alpha_1$ R66C $\beta_2$	5540 $\pm$ 210	554	6	<i>n.d.</i>		<i>n.d.</i>	
$\alpha_1$ S68C $\beta_2$	6.5 $\pm$ 0.5	0.65	5	10.0 $\pm$ 0.3	2	46 $\pm$ 5	3
$\alpha_1$ T129C $\beta_2$	136 $\pm$ 6	13.6	6	<i>n.d.</i>		<i>n.d.</i>	

**Table 6**

Extent of inhibition of GABA-induced currents after reaction with MTS reagent.

	$\alpha_1$ F64C	$\alpha_1$ R66C	$\alpha_1$ S68C	$\alpha_1$ T129C
MTSES <sup>-</sup>	89 ± 3 (4)	62 ± 3 (4)	60 ± 10 (3)	n. d.
MTSEA-biotin	n. d.	75 ± 4 (9)	n. d.	60 ± 3 (6)

Inhibition (% ± S.E.M. (n)) for GABA EC<sub>50</sub> currents after complete reaction with MTSES<sup>-</sup> and MTSEA-biotin on GABA<sub>A</sub> receptors containing the cited cys-engineered  $\alpha_1$  subunit together with the  $\beta_2$  subunit expressed in *Xenopus* oocytes. n.d. = not determined.

**Table 7**

MTS-reagent reaction rates.

Receptor	MTS-reagent	Reaction Rate [ $M^{-1}/s$ ]	n
$\alpha_1$ F64C $\beta_2$	MTSES <sup>-</sup>	11,300 $\pm$ 700	3
$\alpha_1$ R66C $\beta_2$	MTSES <sup>-</sup>	48 $\pm$ 7	5
$\alpha_1$ S68C $\beta_2$	MTSEA-biotin	5500 $\pm$ 1600	6
$\alpha_1$ T129C $\beta_2$	MTSES <sup>-</sup>	240 $\pm$ 40	4
	MTSEA-biotin	6,700,000 $\pm$ 1,100,000	3